

A new class of non-stationary Gaussian fields with general smoothness on metric graphs

David Bolin*, Lenin Riera-Segura*, and Alexandre B. Simas*
 Statistics Program, Computer, Electrical and Mathematical
 Sciences and Engineering (CEMSE) Division,
 King Abdullah University of Science and Technology (KAUST),
 Thuwal, 23955-6900, Kingdom of Saudi Arabia

Abstract

The increasing availability of network data has driven the development of advanced statistical models specifically designed for metric graphs, where Gaussian processes play a pivotal role. While models such as Whittle–Matérn fields have been introduced, there remains a lack of practically applicable options that accommodate flexible non-stationary covariance structures or general smoothness. To address this gap, we propose a novel class of generalized Whittle–Matérn fields, which are rigorously defined on general compact metric graphs and permit both non-stationarity and arbitrary smoothness. We establish new regularity results for these fields, which extend even to the standard Whittle–Matérn case. Furthermore, we introduce a method to approximate the covariance operator of these processes by combining the finite element method with a rational approximation of the operator’s fractional power, enabling computationally efficient Bayesian inference for large datasets. Theoretical guarantees are provided by deriving explicit convergence rates for the covariance approximation error, and the practical utility of our approach is demonstrated through simulation studies and an application to traffic speed data, highlighting the flexibility and effectiveness of the proposed model class.

Keywords: Gaussian process, finite element method, rational approximation, covariance operator, non-stationary model

1 Introduction

In recent years, the ever-increasing availability of data collected from networks such as streets or water systems has encouraged researchers to propose and develop new statistical models for the analysis of network data (Borovitskiy et al., 2021; Bolin et al., 2023a; Cressie et al., 2006; Ver Hoef et al., 2006). A network of this type can be conveniently represented by a metric graph, which is a graph equipped with a notion of distance and where the edges

*The authors are listed alphabetically.

are curves that connect the vertices (Berkolaiko and Kuchment, 2013). The difference from a combinatorial graph is thus that the edges are not only connecting the vertices, but are curves on which we want to define statistical models. An example of a simple metric graph and a simulated non-stationary process on it can be seen in Figure 1.

As in Euclidean domains, the formulation of Gaussian processes is foundational for the development of new statistical models on metric graphs. For practical applications, it is typically important that the class of Gaussian processes allows for

- (i) processes with different smoothness, and the smoothness can be estimated from data. This is in particular important if the model is used for spatial prediction (Stein, 1999; Kirchner and Bolin, 2022; Geoga et al., 2023; De Oliveira and Han, 2022);
- (ii) non-stationary covariance functions, where important characteristics such as marginal variances and practical correlation ranges can vary across the space. This is in particular important when modeling data over large spatial domains (Bolin et al., 2024);
- (iii) computationally efficient inference and prediction, so that it can be applied to large data sets (Lindgren et al., 2011).

There have been several attempts to define Gaussian processes on metric graphs. An early example of these can be found in Ver Hoef et al. (2006) which studied Gaussian processes specifically designed for river networks. More recently, Anderes et al. (2020) defined Gaussian processes with valid isotropic covariance functions for graphs with Euclidean edges. Their approach has later been extended to spatio-temporal models (Porcu et al., 2023; Filosi et al., 2023) and log-Gaussian Cox processes (Møller and Rasmussen, 2024). However, the restriction to have Euclidean edges, for example, excludes graphs where multiple edges connect the same two vertices and can be rather restrictive for real applications. One instance where this is evident is the application we will present later, which is defined on a graph that does not have Euclidean edges (see Figure 10). Other drawbacks of these models are that they cannot be used to model differentiable processes (which thus is a restriction to our first requirement of allowing for difference smoothness), and they are by construction isotropic and can therefore not model non-stationarity.

Other attempts to define Gaussian processes for data on metric graphs can be found in Borovitskiy et al. (2021) and Sanz-Alonso and Yang (2022), where both used models based on the so-called graph Laplacian. However, contrary to the Gaussian processes proposed by Anderes et al. (2020), these processes are defined only on the vertices.

Recently, Bolin et al. (2024a) introduced the Whittle-Matérn fields as a class of Gaussian processes specified as solutions u to the following fractional order differential equation

$$(\kappa^2 - \Delta_\Gamma)^{\alpha/2}(\tau u) = \mathcal{W}, \quad \text{on } \Gamma, \quad (1)$$

for a metric graph Γ , where Δ_Γ is the so-called Kirchhoff-Laplacian (see later sections for details), $\tau, \kappa > 0$ control the marginal variance and practical correlation range, respectively, $\alpha > 1/2$ controls the smoothness, and \mathcal{W} is Gaussian white noise defined on a probability space $(\Omega, \mathcal{F}, \mathbb{P})$. Defining the Whittle-Matérn fields in this way is motivated by the fact that when this equation is considered on \mathbb{R}^p (and Δ_Γ is replaced by the standard Laplacian), the solution u is a centered Gaussian random field with an isotropic Matérn covariance function (Matérn, 1960). Thus, the Whittle-Matérn fields is a natural metric graph analogue to

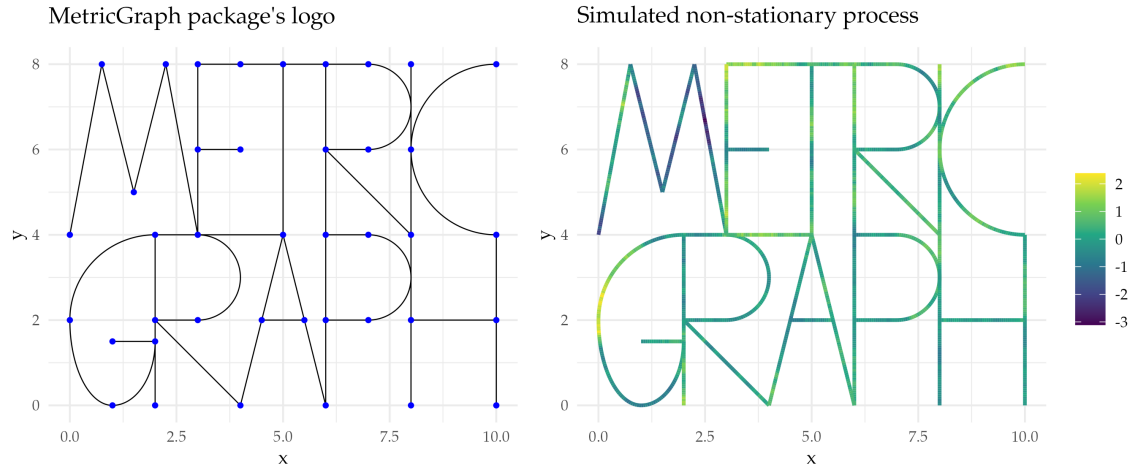


Figure 1: `MetricGraph` package's logo and a simulated non-stationary process on it.

Gaussian processes with Matérn covariance functions on \mathbb{R}^d and they possess some desirable properties. For instance, they are specified on the entire metric graph (not only on the vertices) and are, in fact, well-defined for any compact metric graph. Furthermore, they can model fields of different smoothness and, for example, have differentiable sample paths whenever $\alpha > 3/2$. Bolin et al. (2023a) showed that computationally efficient inference can be performed for these models whenever $\alpha \in \mathbb{N}$, and that having differentiable processes can be very beneficial for spatial prediction.

Bolin et al. (2024) later showed that these fields can be generalized to have non-stationary covariance functions by considering a more general differential operator in (1). Specifically, they introduced the so-called Generalized Whittle-Matérn fields as solutions to the differential equation $L^{\alpha/2}u = \mathcal{W}$ where L is a second order elliptic operator given by $L = \kappa^2 - \nabla(H\nabla)$ for sufficiently smooth functions κ and H . They showed that one can sample these models approximately by using a combination of the finite element method (FEM) and a quadrature approximation of the fractional power of the operator. These fields thus satisfy the first two requirements listed above. However, Bolin et al. (2024) did not consider statistical inference for these models, and their numerical approximation is not suitable for statistical applications as it is computationally demanding and incompatible with popular inference tools such as `R-INLA` (Lindgren and Rue, 2015). See Bolin et al. (2024) for a discussion about this for models on Euclidean domains.

In this work, we propose a version of the Generalized Whittle-Matérn fields, defined through the equation (1) but where both κ and τ are allowed to be spatially varying functions. An advantage of this model compared to those considered by Bolin et al. (2024) is that they provide more direct control over marginal variances and local practical correlation ranges, and they can be viewed as the metric graph analogue of the non-stationary SPDE-based models originally proposed by Lindgren et al. (2011) for Euclidean domains and manifolds. As an important special case of the model class, we introduce the variance-stationary Whittle-Matérn fields, which are defined so that they have constant variance throughout the domain. For the proposed model class, we introduce a computationally efficient approximation which is suitable for Bayesian or likelihood-based inference. The method is theoretically justified by deriving explicit convergence rates for the covariance

function of the approximation and we show how to use it for computationally efficient inference. The method is illustrated through simulation experiments and an application to traffic speed observations, where we show that the ability to estimate the smoothness from data and model non-stationarity greatly improves the predictive power.

The remainder of the paper is organized as follows. Section 2 provides preliminary concepts and notation, defines the model class, and illustrates key properties of the model. Section 3 introduces the numerical approximation method and its properties. In Section 4, we perform numerical experiments to show the accuracy of the proposed approximation and to verify the theoretical results. Finally, Section 5 is devoted to the application and some final conclusions are given in Section 6. Technical details, proofs and further simulation results can be found in the appendices in the Supplementary Materials. The proposed model and the approximation methods are implemented in the `MetricGraph` package (Bolin et al., 2023d), available on CRAN. This package facilitates using the models in general latent Gaussian models which can be fitted to data using `R-INLA`.

2 A class of non-stationary Gaussian random fields

2.1 Preliminaries

First, let us provide the exact definition of a metric graph and introduce some notation. A compact metric graph is a pair $\Gamma = (\mathcal{V}, \mathcal{E})$, where $\mathcal{V} = \{v\}$ is a finite set of vertices and $\mathcal{E} = \{e\}$ is a finite set of undirected edges that are rectifiable curves. The graph is equipped with a metric $d(\cdot, \cdot)$, which we assume is the geodesic distance. We further assume that Γ is *connected* so that there is a path between any two points in Γ . Each edge $e \in \mathcal{E}$ has a positive length $\ell_e \in (0, \infty)$ and connects two vertices \underline{e} and \bar{e} in \mathcal{V} . A point $s \in \Gamma$ can therefore be represented as $s = (e, t)$, where the first coordinate indicates the edge and the second coordinate indicates the distance $t \in [0, \ell_e]$ from \underline{e} . For each vertex $v \in \mathcal{V}$, we let \mathcal{E}_v denote the set of edges incident to v , and let $d_v = |\mathcal{E}_v|$ denote the degree of v .

A real-valued function f on Γ is a collection of functions $(f_e)_{e \in \mathcal{E}}$, each defined on an edge $e \in \mathcal{E}$, i.e., $f_e : [0, \ell_e] \rightarrow \mathbb{R}$. Note that each edge e is identified with its parameterization in the interval $[0, \ell_e]$, and for each edge $e \in \mathcal{E}$, $f_e = f|_e$. An essential class of functions in the context of Gaussian processes is the space of square-integrable functions, $L_2(\Gamma)$, defined as functions that are square integrable on each edge of the graph. This space is equipped with an inner product $(f, g)_{L_2(\Gamma)} = \int_{\Gamma} f(s)g(s)ds = \sum_{e \in \mathcal{E}} \int_e f_e(s)g_e(s)ds$ and induced norm $\|f\|_{L_2(\Gamma)}^2 = \sum_{e \in \mathcal{E}} \|f_e\|_{L_2(e)}^2$, where $f = (f_e)_{e \in \mathcal{E}}$, $g = (g_e)_{e \in \mathcal{E}} \in L_2(\Gamma)$, and $L_2(e)$ denotes the standard Lebesgue space on the interval $[0, \ell_e]$.

We let $C(\Gamma)$ denote the space of continuous functions on Γ , equipped with the norm $\|f\|_{C(\Gamma)} = \sup_{s \in \Gamma} |f(s)|$, and let $L^\infty(\Gamma)$ denote the space of essentially bounded functions, with norm $\|f\|_{L^\infty(\Gamma)} = \text{ess sup}_{s \in \Gamma} |f(s)|$. Additionally, we consider the space of γ -Hölder continuous functions, $C^{0,\gamma}(\Gamma)$, for $0 < \gamma \leq 1$, with seminorm $[f]_{C^{0,\gamma}(\Gamma)} = \sup_{s, s' \in \Gamma} \frac{|f(s) - f(s')|}{d(s, s')^\gamma}$, and norm $\|f\|_{C^{0,\gamma}(\Gamma)} = \|f\|_{C(\Gamma)} + [f]_{C^{0,\gamma}(\Gamma)}$. On individual edges, which are identified with compact intervals of the real line, these function spaces coincide with their standard definitions. Specifically, $C(e)$ denotes the space of continuous functions, while for $0 < \gamma \leq 1$, $C^{0,\gamma}(e)$ denotes the space of γ -Hölder continuous functions, and $C^{1,\gamma}(e)$ denotes the space of continuously differentiable functions whose derivatives are γ -Hölder continuous. Notably, a

γ -Hölder continuous function with $\gamma = 1$ is referred to as a Lipschitz function. For further details, see Appendices A and B.

2.2 The model class

As previously mentioned, we consider Gaussian fields specified as solutions to (1) when κ and τ are functions which will determine the marginal variances and practical correlation ranges of the process. To guarantee the existence of these processes, we make the following weak assumptions on κ and τ .

Assumption 1. *We assume that $\kappa, \tau \in L_\infty(\Gamma)$ and that there exist $\kappa_0, \tau_0 > 0$ such that $\text{ess inf}_{s \in \Gamma} \kappa(s) \geq \kappa_0$ and $\text{ess inf}_{s \in \Gamma} \tau(s) \geq \tau_0$.*

We now formally define the model. The Kirchhoff–Laplacian in (1) is a differential operator that acts on a function f by taking its second derivative on each edge, provided that f_e has a well-defined second derivative on every edge e . The operator is coupled with the following vertex conditions, known as Kirchhoff’s vertex conditions:

$$f \text{ is continuous on } \Gamma \text{ and satisfies } \sum_{e \in \mathcal{E}_v} \partial_e f(v) = 0 \text{ for every } v \in \mathcal{V}, \quad (2)$$

where $\partial_e f(v)$ is the derivative of f_e at the vertex v , taken in the direction outward from v .

Given $L = \kappa^2 - \Delta_\Gamma$, the fractional power L^α , for $\alpha > 0$, is defined in the spectral sense. This definition is valid because L is a densely defined, self-adjoint operator with a compact resolvent, ensuring a well-posed spectral decomposition. In particular, the inverse fractional power $L^{-\alpha}$ is also well-defined. For further details, see Appendix C.

The final component needed to understand (1) is the definition of Gaussian white noise. It is represented as a family of centered Gaussian random variables $\{\mathcal{W}(h) : h \in L_2(\Gamma)\}$ satisfying $\mathbb{E}[\mathcal{W}(h)\mathcal{W}(g)] = (h, g)_{L_2(\Gamma)}$ for all $h, g \in L_2(\Gamma)$. A solution to (1) is a centered Gaussian random field u in $L_2(\Gamma)$ satisfying, for all $h \in L_2(\Gamma)$, $(u, h)_{L_2(\Gamma)} = \mathcal{W}(L^{-\alpha/2}(\tau^{-1}h))$, where $\tau^{-1}h$ is the function defined by $(\tau^{-1}h)(s) = \tau^{-1}(s)h(s)$ for all $s \in \Gamma$. For further details, refer to Appendix C. The following result shows the existence of a solution to (1).

Proposition 1. *Let $1/2 < \alpha \leq 2$. If Assumption 1 holds, (1) has a unique solution u which is a centered Gaussian process with a strictly positive definite covariance function $\varrho^\alpha(s, t) = \text{Cov}(u(s), u(t))$.*

The main difficulty in proving this novel result is to show the strict positive definiteness of ϱ^α . However, this is a highly useful property for statistical applications.

2.3 Regularity of the field

As mentioned in the introduction, a key property of Gaussian random fields is their ability to exhibit varying degrees of regularity. While the existence result in the previous section establishes the existence of solutions, it does not address their smoothness. Our goal here is to investigate the regularity of these solutions. The parameter α plays a critical role in determining regularity; however, due to the way τ appears in (1), additional assumptions on τ are required to achieve a desired level of regularity. This observation is particularly relevant for practical applications, as we will illustrate later.

We distinguish between two types of regularity: *local regularity*, which examines the regularity of the field when restricted to individual edges, and *global regularity*, which considers the regularity across the entire metric graph. The main result concerning local regularity is presented below. In the result and later, when we state that a Gaussian process u belongs to a function space F we mean that there exists a modification of u such that the sample paths of the modified field belong to F .

Proposition 2. *Let u be the solution to (1) under Assumption 1, with $1/2 < \alpha \leq 2$. Define $\tilde{\alpha} = \min\{\alpha - 1/2, 1/2\}$. Then:*

- (i) *If $\alpha > 1/2$, then for any γ such that $0 < \gamma < \tilde{\alpha}$ and $\tau_e \in C^{0,\gamma}(e)$ for all $e \in \mathcal{E}$, we have $u_e \in C^{0,\gamma}(e)$ for every $e \in \mathcal{E}$.*
- (ii) *If $\alpha > 3/2$, then for any γ such that $0 < \gamma < \tilde{\alpha} - 1$ and $\tau_e \in C^{1,\gamma}(e)$ for all $e \in \mathcal{E}$, we have $u_e \in C^{1,\gamma}(e)$ for every $e \in \mathcal{E}$.*

We now consider global regularity by imposing additional assumptions on τ .

Proposition 3. *Under the same setting as Proposition 2:*

- (i) *If $\alpha > 1/2$ and for some $\gamma \in (0, \tilde{\alpha})$ we have $\tau_e \in C^{0,\gamma}(e)$ for all $e \in \mathcal{E}$, then $u \in C(\Gamma)$ whenever $\tau \in C(\Gamma)$. Furthermore, if $\tau \in C^{0,\gamma}(\Gamma)$, then $u \in C^{0,\gamma}(\Gamma)$. Conversely, if $u \in C(\Gamma)$, then $\tau \in C(\Gamma)$.*
- (ii) *If $\alpha > 3/2$ and for some $\gamma \in (0, \tilde{\alpha} - 1)$ we have $\tau_e \in C^{1,\gamma}(e)$ for all $e \in \mathcal{E}$, and τ satisfies the Kirchhoff conditions (2), then u also satisfies the Kirchhoff conditions.*

We emphasize that the results presented in Proposition 2 and Proposition 3 are novel. In particular, Proposition 3.ii is new even in the context of standard Whittle–Matérn fields as it improves upon Bolin et al. (2024a, Proposition 11), where $\alpha \geq 2$ was required for standard Whittle–Matérn fields. Here, we relax this condition to $\alpha > 3/2$.

The dependence of the global regularity of the solution on the global regularity of τ is, to the best of our knowledge, a completely novel phenomenon, and it plays a particularly critical role in the context of metric graphs. Unlike in the Euclidean setting, where boundary extensions can often mitigate boundary effects, vertex conditions on metric graphs are unavoidable. Moreover, as α increases, achieving the desired regularity requires increasingly stringent conditions on τ . In contrast, no such additional constraints are imposed on κ , highlighting the importance of careful modeling of τ in practical applications.

To illustrate this, consider the graph in Figure 2. Let $f(s) = \text{edge.number}(s)/4$ and $g(s) = 0.5 \cdot (x^2(s) - y^2(s)) + 0.5$, where $(x(s), y(s))$ are Euclidean coordinates on the plane. A simulation of the Gaussian process u with $\alpha = 3$ is shown in the top row of the figure, with $\tau(s) = \exp(g(s))$ and $\kappa(s) = \exp(f(s))$. In this case, the field is continuous. However, when $\tau(s) = \exp(f(s))$ and $\kappa(s) = \exp(g(s))$, the simulated field is discontinuous, as illustrated in the bottom row of the figure.

2.4 Illustrations of the model properties

To illustrate the flexibility of the proposed model, consider the `MetricGraph` package’s logo in Figure 1. To visualize the versatility of our method in terms of non-stationarity, consider

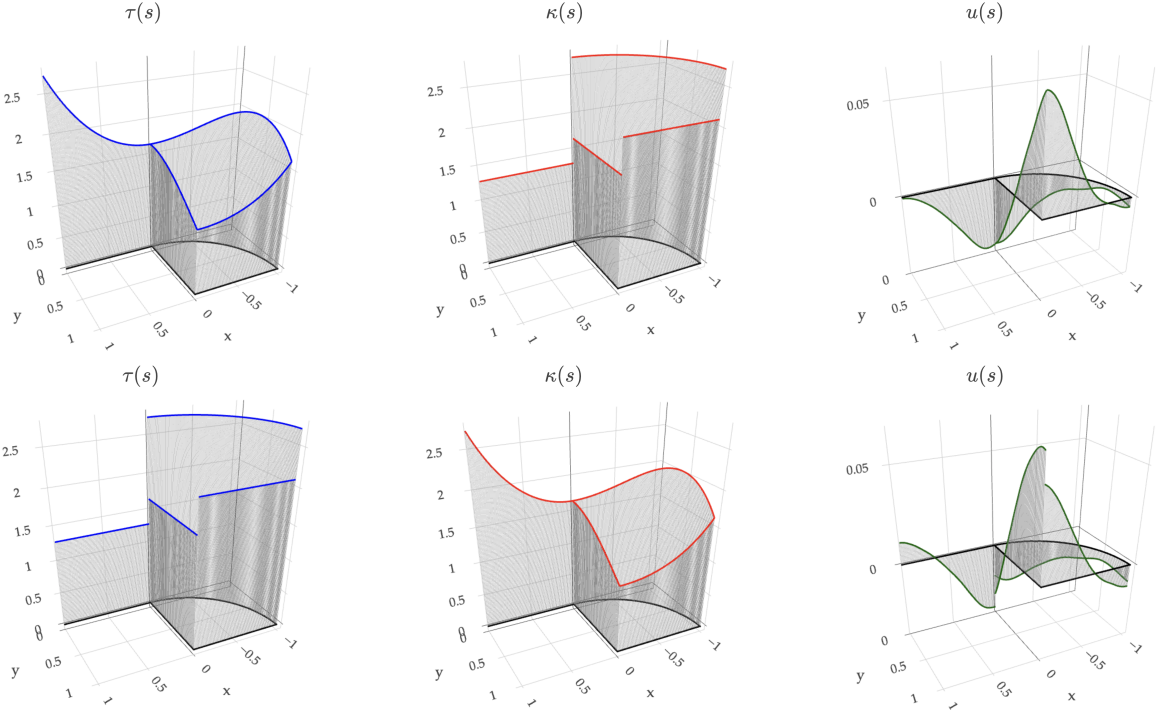


Figure 2: Models for $\tau(s)$ (left), $\kappa(s)$ (center), and their simulated fields $u(s)$ (right).

$\tau(s) = \exp(0.05 \cdot (x(s) - y(s)))$ and $\kappa(s) = \exp(0.1 \cdot (x(s) - y(s)))$, where $(x(s), y(s))$ are Euclidean coordinates on the plane. These choices make $\tau(\cdot)$ and $\kappa(\cdot)$ large in the bottom-right region of the `MetricGraph` package’s logo, as seen from the top row of Figure 3. The bottom row of Figure 3 shows the standard deviation $\sigma(\cdot)$ and practical correlation range $\rho(\cdot)$ (here $\rho(s)$ is the smallest distance $d(s, t)$ so that the correlation between $u(s)$ and $u(t)$ is below 0.1) for the case $\alpha = 0.9$. The panels in the bottom row of Figure 3 also show three locations, s_1, s_2 , and s_3 , which are the same locations as in the left panel of Figure 4, for which we plot $r_i(\cdot) = \varrho^\alpha(s_i, \cdot)$, $i = 1, 2, 3$. We can clearly see that $\sigma(s_i)$ controls the magnitude of $r_i(\cdot)$ and $\rho(s_i)$ controls how quickly the function decays away from s_i . The right panel in Figure 1 shows a simulation of a non-stationary field using the aforementioned choices of $\alpha, \tau(\cdot)$, and $\kappa(\cdot)$. To demonstrate the adaptability of our method concerning general smoothness, let $\tau(\cdot)$ and $\kappa(\cdot)$ as before, and with these fixed, consider three cases for the smoothness parameter, $\alpha = 0.9, 1.3, 2.1$. The right panel of Figure 4 shows an illustration of $\varrho^\alpha(s_0, s)$ for a fixed location s_0 for these choices of α .

2.5 Variance-stationary Whittle–Matérn fields

One feature of the Whittle–Matérn fields on metric graphs is that they are inherently non-isotropic (Bolin et al., 2024a). Their marginal variances and practical correlation ranges change over the graph even if κ and τ are constants. That the practical correlation range is non-stationary is often realistic for applications (Bolin et al., 2024a); however, a non-constant variance might be less ideal in some applications. An example of the marginal standard deviations of a Whittle–Matérn field with $\alpha = 1, \kappa = 2$, and $\tau = 0.5$, on a simple graph are shown in Figure 5. One can note that the variance is higher close to vertices of

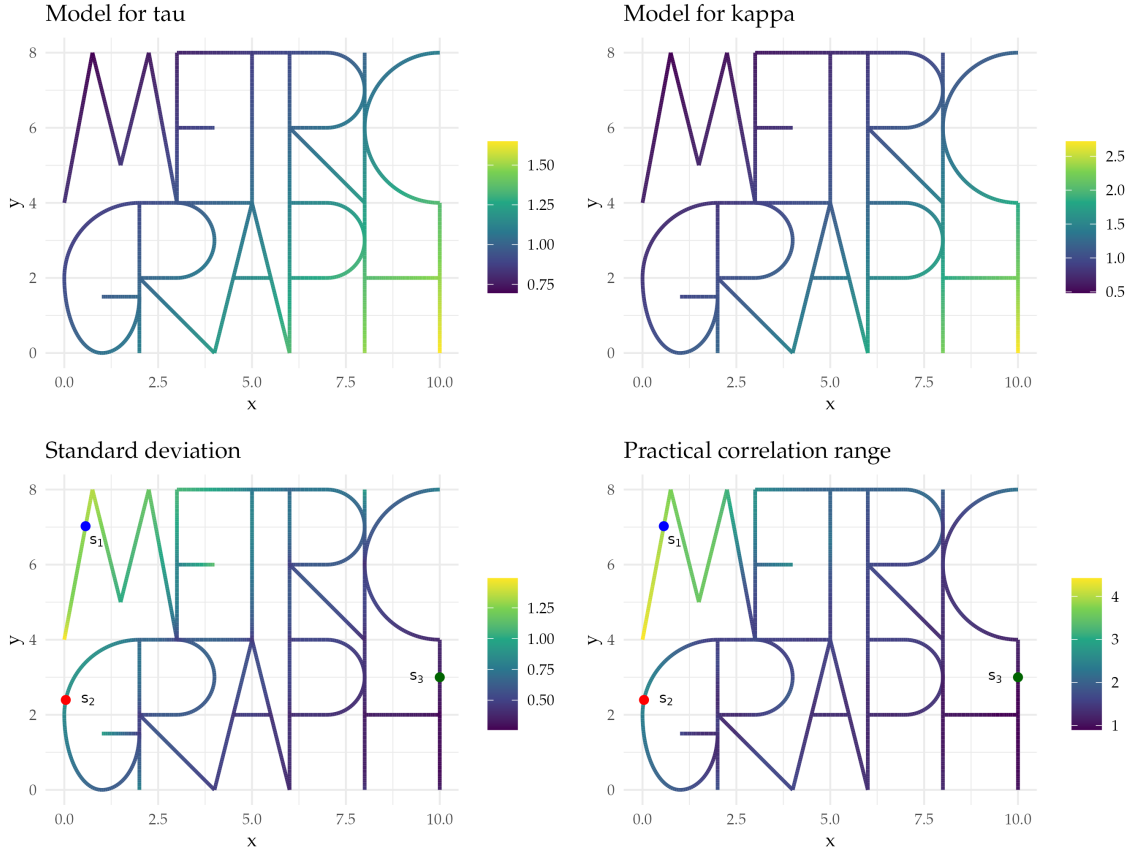


Figure 3: Top row: Non-stationary models for $\tau(\cdot)$ and $\kappa(\cdot)$. Bottom row: Non-stationary standard deviation and practical correlation range on the `MetricGraph` package’s logo.

degree 1 and lower close to vertices of degree larger than two.

An interesting option to mitigate this effect is a non-stationary model defined through

$$(\kappa^2 - \Delta_\Gamma)^{\alpha/2}(\sigma_\kappa u) = \sigma_0 \mathcal{W}, \quad \text{on } \Gamma, \quad (3)$$

where $\sigma_0 > 0$ and $\alpha > 1/2$ are constants, κ satisfies Assumption 1, and $\sigma_\kappa(s)$ represents the marginal standard deviations of a generalized Whittle–Matérn field with the same κ and α , but with $\tau = 1$. This is a special case of (1) with $\tau(s) = \sigma_0^{-1} \sigma_\kappa(s)$. Under this specification, the model parameters are $(\kappa, \sigma_0, \alpha)$, and it follows directly that the variance of $u(s)$ is σ_0^2 for all $s \in \Gamma$. For this reason, we refer to this model as a *variance-stationary Whittle–Matérn field*. The right panel of Figure 5 illustrates the marginal variance of the field for $\sigma_0 = 1$, showing that the variance is indeed 1 across all locations. The following result demonstrates that this choice of τ satisfies a global regularity assumption.

Proposition 4. *Let $1/2 < \alpha \leq 2$, κ satisfy Assumption 1, and $\tau(s) = \sigma_0^{-1} \sigma_\kappa(s)$ for some $\sigma_0 > 0$. Then, $\tau(\cdot)$ satisfies Assumption 1. Further, let u be the solution to (3), then*

- (i) $\tau \in C^{0, \tilde{\alpha}}(\Gamma)$, where $\tilde{\alpha} = \min\{\alpha - 1/2, 1/2\}$, and $u \in C^{0, \gamma}(\Gamma)$ for every $0 < \gamma < \tilde{\alpha}$.
- (ii) If $\alpha > 3/2$, then for every $e \in \mathcal{E}$, $\tau_e \in C^{1, \alpha - 3/2}(e)$, and τ satisfies the Kirchhoff conditions in (2). Consequently, the solution u also satisfies the Kirchhoff conditions.

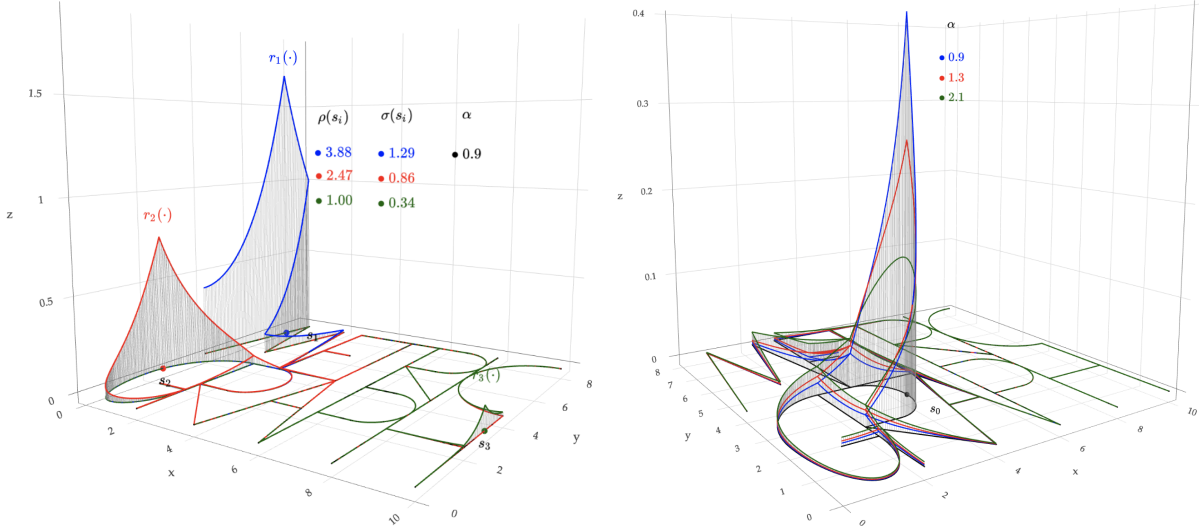


Figure 4: Left: Covariance functions $\rho^\alpha(s_i, s)$, $i = 1, 2, 3$ for three locations of the model with κ and τ as shown in Figure 3 and $\alpha = 0.9$. Right: Covariance functions $\rho^\alpha(s_0, s)$ for different smoothness parameters α .

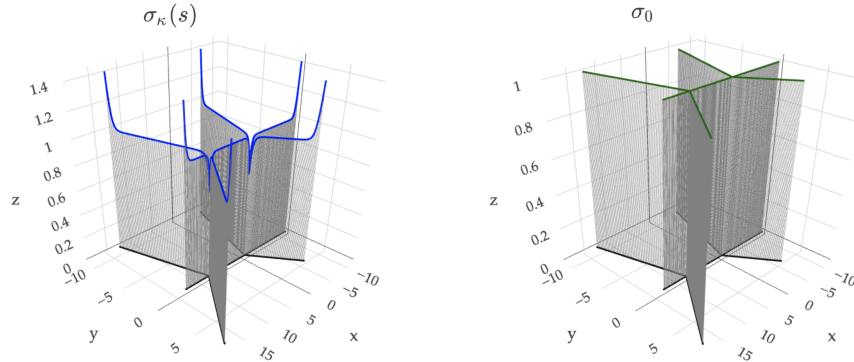


Figure 5: Marginal standard deviation $\sigma_\kappa(\cdot)$ of a Whittle–Matérn field with $\alpha = 1$, $\kappa = 2$, $\tau = 0.5$ (left), and of a Generalized Whittle–Matérn field with $\tau(\cdot) = \sigma_\kappa(\cdot)$ (right).

Implementing the variance-stationary Whittle–Matérn field requires computing $\sigma_\kappa(\cdot)$, which for integer values of α , and constant κ , can be done computationally efficiently using Bolin et al. (2023a, Theorem 4). For non-integer α , we can instead compute $\sigma_\kappa(\cdot)$ based on the numerical approximation method developed in the next section. Based on that approximation, $\sigma_\kappa(\cdot)$ can be obtained through a partial inverse of the precision matrix of the field evaluated at the finite element mesh. The partial inverse can be computed efficiently using the Takahashi equations (Takahashi et al., 1973).

Thus, these variance-stationary fields could serve as flexible alternatives to the isotropic models of Anderes et al. (2020), as they are well-defined for general metric graphs and facilitate computationally efficient inference for fields with general smoothness.

2.6 Non-stationary models with log-regressions for κ and τ

Lindgren et al. (2011) proposed modeling κ and τ in the SPDE approach for Euclidean

domains using log-regressions. Naturally, we can use the same idea for the metric graph models. Specifically, we use covariates $g_1, \dots, g_m \in L_2(\Gamma)$, with $m \in \mathbb{N}$, and define

$$\log \tau(s) = \theta_{\tau,0} + \sum_{j=1}^m \theta_{\tau,j} g_j(s), \quad \log \kappa(s) = \theta_{\kappa,0} + \sum_{j=1}^m \theta_{\kappa,j} g_j(s), \quad s \in \Gamma, \quad (4)$$

where $\theta_{\tau,0}, \dots, \theta_{\tau,m} \in \mathbb{R}$ and $\theta_{\kappa,0}, \dots, \theta_{\kappa,m} \in \mathbb{R}$ are unknown parameters to be estimated. A natural question is then what assumptions we have to make on the covariates to ensure the regularity requirements of Proposition 3. Because the main requirement there is on τ , the following proposition shows how τ inherits the regularity of the covariates.

Proposition 5. *Let τ be defined by (4), where $m \in \mathbb{N}$ and $g_1, \dots, g_m \in C^{0,\gamma}(\Gamma)$ for some $0 < \gamma \leq 1$. Then, $\tau \in C^{0,\gamma}(\Gamma)$. Furthermore, if $g_{1,e}, \dots, g_{m,e} \in C^{1,\gamma}(e)$ for every $e \in \mathcal{E}$, and each g_j satisfies the Kirchhoff conditions (2) for $j = 1, \dots, m$, then $\tau_e \in C^{1,\gamma}(e)$, and τ also satisfies the Kirchhoff conditions (2).*

A common scenario is that some covariate of interest, $Z(s)$, is only available at some fixed locations $s_1, \dots, s_n \in \Gamma$. To obtain a continuously indexed covariate, we can use kriging prediction to interpolate the observed values z_1, \dots, z_n . We can do this by either assuming that the observed values are direct observations of the covariate, $z_i = Z(s_i)$, or by assuming that they are noisy observations of the covariate,

$$z_i | Z(\cdot) \sim N(Z(s_i), \sigma_\epsilon^2), \quad i = 1, \dots, n, \quad \sigma_\epsilon^2 > 0. \quad (5)$$

In either case, to perform the interpolation, we assume that $Z(s) = \beta_0 + w(s)$, where $\beta_0 \in \mathbb{R}$ is an intercept, and $w(\cdot)$ is a centered Gaussian process obtained as the solution to

$$(\kappa^2 - \Delta_\Gamma)^{\alpha/2} w = \sigma_0 \mathcal{W}, \quad \sigma_0 > 0. \quad (6)$$

We then fit this model to the observed values and use $z(s) = \beta_0 + \mathbb{E}(w(s) | z_1, \dots, z_n)$, $s \in \Gamma$ as the covariate. The next proposition establishes the regularity of this covariate.

Proposition 6. *Let $1/2 < \alpha \leq 2$, and let w be the solution to (6). Assume that z_1, \dots, z_n either are direct observations of $Z(s)$ or follow (5), where $\beta_0 > 0$, $n \in \mathbb{N}$, $\sigma_\epsilon > 0$, and $s_1, \dots, s_n \in \Gamma$ are distinct locations. Finally, let $z(s) = \beta_0 + \mathbb{E}(w(s) | z_1, \dots, z_n)$.*

- (i) *If $\alpha > 1/2$, for any $0 < \gamma \leq \tilde{\alpha}$, with $\tilde{\alpha} = \min\{\alpha - 1/2, 1/2\}$, we have $z \in C^{0,\gamma}(\Gamma)$.*
- (ii) *If $\alpha > 3/2$, for any $0 < \gamma \leq \alpha - 1/2$, we have $z_e \in C^{1,\gamma}(e)$ for every $e \in \mathcal{E}$, and z satisfies the Kirchhoff conditions (2).*

By combining Propositions 5 and 6, we conclude that a log-regression model for τ using a kriging predictor as a covariate ensures the regularity conditions required in Proposition 3.

3 The numerical approximation method

Having defined the models and illustrated their flexibility, it remains to obtain a method for using them in statistical inference. In this section, we outline the main idea of this method, show the main theoretical results, and finally illustrate how the approximation is used for computationally efficient inference.

3.1 Main idea

Bolin et al. (2023a) showed that one can evaluate finite-dimensional distributions exactly and computationally efficiently of solutions to (1) whenever $\kappa, \tau > 0$ are constants and $\alpha \in \mathbb{N}$. Their approach relies heavily on the fact that the corresponding process has Markov properties (Bolin et al., 2024b) whenever $\alpha \in \mathbb{N}$. As we want a method that works for general $\alpha > 1/2$, there is little hope in extending their method to the non-stationary fields that we are considering here. Bolin et al. (2024) proposed approximating Generalized Whittle–Matérn fields using the finite element approach combined with a quadrature approximation of the fractional power of the operator. That is essentially the metric graph version of the rational SPDE approach proposed in Bolin and Kirchner (2020) for the corresponding Generalized Whittle–Matérn fields on Euclidean domains. The disadvantage of this approach is that the corresponding approximation is not a Gaussian Markov random field (GMRF), which means that it cannot be implemented in software such as R-INLA (Bolin et al., 2024). This limits applicability, as the vast majority of applications of the SPDE approach have been done using R-INLA, because of its flexibility and computational efficiency. For Euclidean domains, Bolin et al. (2024) solved this issue by proposing the covariance-based rational SPDE approach, where they directly performed a rational approximation of the covariance operator of the process to obtain a GMRF approximation. The method we propose for the non-stationary Gaussian processes on metric graphs is the metric graph version of this approach. Specifically, we first perform a FEM approximation and then a rational approximation of the corresponding covariance operator.

3.2 Finite element approximation

To construct the finite element approximation, we introduce a space of piecewise linear and continuous functions, V_h , which is spanned by a set of hat functions $\{\psi_j\}_{j=1}^{N_h}$ on the graph. This set is obtained by introducing internal vertices on each edge, and for each vertex we define a basis function that is one at the vertex and decreases linearly to zero at the closest other vertices. We use h to denote the largest distance between any two neighboring vertices, which is a parameter that will control the accuracy of the approximation. An example of the construction can be seen in Figure 6, where we illustrate that the hat functions can be divided into two types, one where the vertex is of degree 2, and one where the vertex is of higher degree. Furthermore, note that for any function $\phi \in V_h$ and every edge $e \in \mathcal{E}$, the function ϕ_e is differentiable almost everywhere on e . The points where ϕ_e is not differentiable form a finite set, corresponding to the “tips” of the hat basis functions. More details on the precise definitions of these functions are provided in Appendix G.

We define the discrete version of L as $L_h : V_h \rightarrow V_h$ via

$$(L_h \phi, \psi)_{L_2(\Gamma)} = \mathfrak{h}(\phi, \psi), \quad \phi, \psi \in V_h.$$

Here \mathfrak{h} is the bilinear form corresponding to the operator L , given by

$$\mathfrak{h}(f, g) = (\kappa^2 f, g)_{L_2(\Gamma)} + \sum_{e \in \mathcal{E}} \int_e f'_e(s) g'_e(s) ds,$$

where the derivatives are the almost everywhere derivatives of f_e and g_e . We now define the corresponding discrete problem for (1), which consists of finding $u_h \in V_h$ such that

$$L_h^{\alpha/2}(\tau u_h) = \mathcal{W}_h, \tag{7}$$

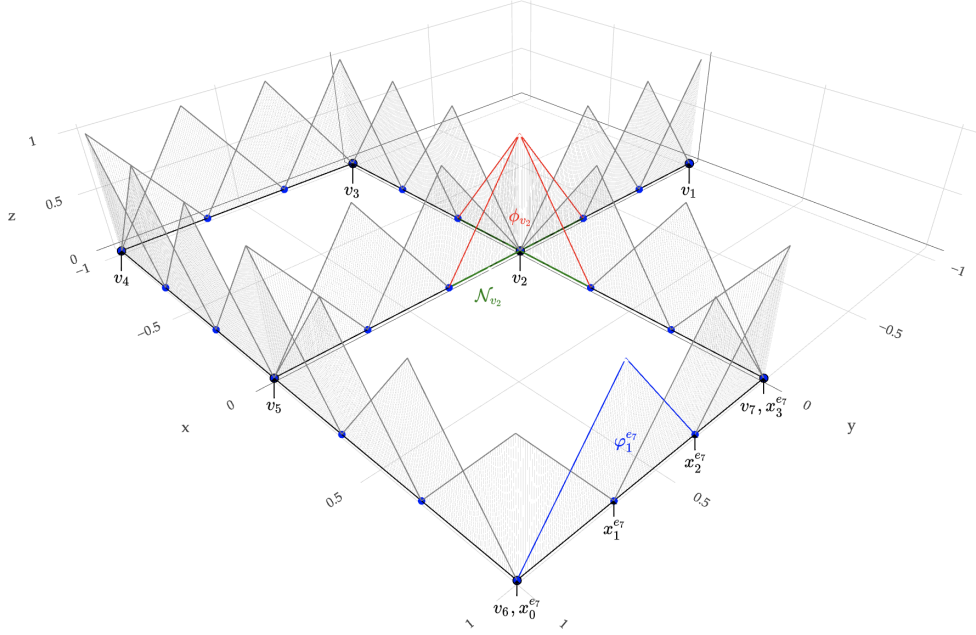


Figure 6: Illustration of the system of basis functions $\{\psi_j\}_{j=1}^{N_h}$ (solid gray lines) on a graph $\Gamma = (\mathcal{V}, \mathcal{E})$ with $\mathcal{E} = \{e_1, \dots, e_8\}$ and $\mathcal{V} = \{v_1, \dots, v_7\}$.

where \mathcal{W}_h represents Gaussian white noise on V_h . Specifically, \mathcal{W}_h can be expressed as a collection of centered Gaussian random variables $\{\mathcal{W}_h(\psi_j)\}_{j=1}^{N_h}$, where ψ_j is the j th hat basis function of V_h . These variables satisfy $\mathbb{E}[\mathcal{W}_h(\psi_i)\mathcal{W}_h(\psi_j)] = (\psi_i, \psi_j)_{L_2(\Gamma)}$, for $i, j = 1, \dots, N_h$. The fractional power of L_h is defined in the spectral sense; further details can be found in Appendix G. The solution of (7) can be represented as

$$u_h(s) = \sum_{j=1}^{N_h} u_j \psi_j(s), \quad (8)$$

To illustrate how this approximation works, let $\alpha = 2$ and $\tau \equiv 1$ in (7). In this case, the stochastic coefficients $\mathbf{u} = [u_1, \dots, u_{N_h}]^\top$ in (8) can be determined by solving the linear system $\mathfrak{h}(u_h, \psi_j) = \mathcal{W}_h(\psi_j)$, $j = 1, \dots, N_h$. In matrix form, this system can be written as $(\mathbf{G} + \mathbf{C}^\kappa)\mathbf{u} = \mathbf{W}$, where \mathbf{G} is the stiffness matrix with entries $\mathbf{G}_{ij} = (\psi'_i, \psi'_j)_{L_2(\Gamma)}$, \mathbf{C}^κ has entries $\mathbf{C}_{ij}^\kappa = (\kappa^2 \psi_i, \psi_j)_{L_2(\Gamma)}$, and $\mathbf{W} = [\mathcal{W}_h(\psi_1), \dots, \mathcal{W}_h(\psi_{N_h})]^\top \sim N(\mathbf{0}, \mathbf{C})$, with \mathbf{C} having entries $\mathbf{C}_{ij} = (\psi_i, \psi_j)_{L_2(\Gamma)}$. It follows that $\mathbf{u} \sim N(\mathbf{0}, \mathbf{Q}_2^{-1})$, where $\mathbf{Q}_2 = \mathbf{L}^\top \mathbf{C}^{-1} \mathbf{L}$ with $\mathbf{L} = \mathbf{G} + \mathbf{C}^\kappa$. In the case that $\tau(\cdot)$ is a spatially varying function and a piecewise constant approximation of $\kappa(\cdot)$ is considered, the precision matrix of \mathbf{u} becomes $\mathbf{Q}_2 = \boldsymbol{\tau} \mathbf{L}^\top \mathbf{C}^{-1} \mathbf{L} \boldsymbol{\tau}$, where $\mathbf{L} = \mathbf{G} + \boldsymbol{\kappa}^2 \mathbf{C}$ with $\boldsymbol{\tau} = \text{diag}(\tau(s_1), \dots, \tau(s_{N_h}))$ and $\boldsymbol{\kappa}^2 = \text{diag}(\kappa^2(s_1), \dots, \kappa^2(s_{N_h}))$. To obtain a sparse precision matrix, one can replace the mass matrix \mathbf{C} by a lumped mass matrix $\tilde{\mathbf{C}}$, which is a diagonal matrix with entries $\tilde{\mathbf{C}}_{ii} = \sum_{j=1}^{N_h} \mathbf{C}_{ij}$.

3.3 Handling the fractional power

To extend the approach to a general value of $\alpha > 1/2$, we extend the covariance-based rational approximation of Bolin et al. (2024) to our metric graph setting. The solution u_h

to the discrete problem has covariance function $\varrho_h^\alpha(\cdot, \cdot)$, which is the kernel of the covariance operator $M_{\tau^{-1}}L_h^{-\alpha}M_{\tau^{-1}}$, where $M_{\tau^{-1}}$ denotes the operator that multiplies a function with τ^{-1} . We approximate this by performing a rational approximation of $L_h^{-\alpha}$. Specifically, for the real-valued function $\hat{f}(x) = x^{\{\alpha\}}$, where $\{x\} = x - \lfloor x \rfloor \in [0, 1)$ denotes the fractional part of x , consider the rational approximation of order m , $\hat{f}(x) \approx \hat{r}_m(x) = p(x)/q(x)$, defined on the interval $[0, \kappa_0^{-2}]$, which contains the spectrum of L_h^{-1} . Here, κ_0 is as specified in Assumption 1, $p(x) = \sum_{i=0}^m a_i x^i$, and $q(x) = \sum_{i=0}^m b_i x^i$, with the coefficients $\{a_i\}$ and $\{b_i\}$ determined as the best rational approximation in the L_∞ -norm. These coefficients can be efficiently computed using the BRASIL algorithm (Hofreither, 2021), see Appendix H for more details. Defining $r_m(x) := x^{\lfloor \alpha \rfloor} \hat{r}_m(x)$, we then approximate

$$L_h^{-\alpha} = L_h^{-\lfloor \alpha \rfloor} L_h^{-\{\alpha\}} \approx L_h^{-\lfloor \alpha \rfloor} p(L_h^{-1}) q(L_h^{-1})^{-1} = L_h^{-\lfloor \alpha \rfloor} \left(\sum_{i=1}^m r_i (L_h - p_i I_{V_h})^{-1} + k I_{V_h} \right),$$

where the coefficients $r_i, k > 0$ and $p_i < 0$ are obtained by performing a partial fraction decomposition of \hat{r} and I_{V_h} is the identity operator on V_h . By Bolin et al. (2024, Appx. C), the covariance matrix of the weights $\mathbf{u} = [u_1, \dots, u_{N_h}]^\top$ in (8) can be written as

$$\Sigma_{\mathbf{u}} = \tau^{-1} (\mathbf{L}^{-1} \mathbf{C})^{\lfloor \alpha \rfloor} \sum_{i=1}^m r_i (\mathbf{L} - p_i \mathbf{C})^{-1} \tau^{-1} + \tau^{-1} \mathbf{K}_{\lfloor \alpha \rfloor} \tau^{-1}, \quad (9)$$

where \mathbf{C} and \mathbf{L} are as before, and $\mathbf{K}_n = k(\mathbf{L}^{-1} \mathbf{C})^{n-1} \mathbf{L}^{-1}$ for $n \in \mathbb{N}$ with $\mathbf{K}_0 = k\mathbf{C}$. Because $r_i, k > 0$ and $p_i < 0$, each term in the expression of $\Sigma_{\mathbf{u}}$ is a valid covariance matrix. We can therefore express \mathbf{u} as a sum of $m + 1$ independent random vectors \mathbf{x}_i ,

$$\mathbf{u} = \sum_{i=1}^{m+1} \mathbf{x}_i, \quad \mathbf{x}_i \sim N(\mathbf{0}, \mathbf{Q}_i^{-1}), \quad (10)$$

where

$$\mathbf{Q}_i = \begin{cases} r_i^{-1} \tau (\mathbf{L} - p_i \mathbf{C}) (\mathbf{C}^{-1} \mathbf{L})^{\lfloor \alpha \rfloor} \tau & \text{if } i = 1, \dots, m \\ \tau \mathbf{K}_{\lfloor \alpha \rfloor}^{-1} \tau & \text{if } i = m + 1 \end{cases}$$

To ensure that each \mathbf{Q}_i is sparse, we replace matrix \mathbf{C} by matrix $\tilde{\mathbf{C}}$, as before.

3.4 Convergence rates

A natural question is now how good the rational approximation is. To answer this, note that $M_{\tau^{-1}} r_m(L_h^{-1}) M_{\tau^{-1}}$ is the covariance operator of the rational approximation, which is associated to a covariance function $\varrho_{h,m}^\alpha(\cdot, \cdot)$ defined on $\Gamma \times \Gamma$ through the following relation:

$$(M_{\tau^{-1}} r_m(L_h^{-1}) M_{\tau^{-1}} f)(s) = \int_{\Gamma} \varrho_{h,m}^\alpha(s, s') f(s') ds'.$$

The following result shows that this covariance function approximates the true covariance at a fixed rate depending on the mesh width h and on the order of the rational approximation m . Here and for future reference, convergence in $L_2(\Gamma \times \Gamma)$ means convergence in the norm

$$\|f\|_{L_2(\Gamma \times \Gamma)}^2 = \int_{\Gamma} \int_{\Gamma} f^2(s, r) ds dr = \sum_{e \in \mathcal{E}} \int_e \int_e f_e^2(s, r) ds dr.$$

Proposition 7. *Under Assumption 1, if $\alpha > 1/2$ then for any $\varepsilon > 0$*

$$\|\varrho^\alpha - \varrho_{h,m}^\alpha\|_{L_2(\Gamma \times \Gamma)} \leq C(h^{\min\{2\alpha-1/2, 2\}-\varepsilon} + 1_{\alpha \notin \mathbb{N}} \cdot h^{-1/2} e^{-2\pi\sqrt{\{\alpha\}m}}), \quad (11)$$

where $C > 0$ is a constant independent of h and m .

We can note that we have two terms in the bound for the error, the first is due to the FEM approximation, and the second is due to the rational approximation. If we choose

$$m = c\lceil(\min\{2\alpha - 1/2, 2\} + 1/2)^2 \log^2(h)/(4\pi^2\{\alpha\})\rceil, \quad (12)$$

we balance these two terms and the total rate convergence rate as a function of the mesh size is $\min\{2\alpha - 1/2, 2\}$ if $\alpha > 1/2$. As the error induced by the rational approximation decreases exponentially fast in m , we rarely have to use a large value of m , which is beneficial in practice as the computational cost increases as we increase m .

3.5 Using the approximation for inference

To illustrate the usage of the approximation, suppose we have observations $\mathbf{y} = [y_1, \dots, y_n]^\top$ at locations $s_1, \dots, s_n \in \Gamma$ of a Generalized Whittle-Matérn field under Gaussian measurement noise. That is, $y_i|u(\cdot) \sim N(u(s_i), \sigma_\epsilon^2)$, $s_i \in \Gamma$, $i = 1, \dots, n$, where $u(\cdot)$ is a solution to (1) on Γ . As previously discussed, the solution $u(\cdot)$ of (7) can be approximated as $u_h(s) = \sum_{j=1}^{N_h} u_j \psi_j(s)$, where ψ_j are FEM basis functions and the vector of stochastic weights $\mathbf{u} = [u_1, \dots, u_{N_h}]^\top$ can be expressed as a sum $\mathbf{u} = \sum_{i=1}^{m+1} \mathbf{x}_i$ of independent GMRFs \mathbf{x}_i , each with sparse precision matrix \mathbf{Q}_i . With this formulation, the aforementioned model can be written hierarchically as $\mathbf{X} \sim N(\mathbf{0}, \mathbf{Q}^{-1})$ and $\mathbf{y}|\mathbf{X} \sim N(\overline{\mathbf{A}}\mathbf{X}, \sigma_\epsilon^2 \mathbf{I})$, where $\mathbf{Q} = \text{diag}(\mathbf{Q}_1, \dots, \mathbf{Q}_{m+1})$, $\mathbf{X} = [\mathbf{x}_1^\top, \dots, \mathbf{x}_{m+1}^\top]^\top$, and $\overline{\mathbf{A}} = [\mathbf{A} \ \cdots \ \mathbf{A}]$ with $\mathbf{A}_{ij} = \psi_j(s_i)$. Because of the sparsity of \mathbf{Q} , statistical inference and spatial prediction can be performed computationally efficient, as demonstrated by Bolin et al. (2024). The kriging predictor can then be efficiently computed as $\boldsymbol{\mu}_{\mathbf{X}|\mathbf{y}} = \mathbf{Q}_{\mathbf{X}|\mathbf{y}}^{-1} \overline{\mathbf{A}}^\top \sigma_\epsilon^{-2} \mathbf{I} \mathbf{y}$, where $\mathbf{Q}_{\mathbf{X}|\mathbf{y}} = \overline{\mathbf{A}}^\top \sigma_\epsilon^{-2} \mathbf{I} \overline{\mathbf{A}} + \mathbf{Q}$. One can fit this model and more complex models by combining the `MetricGraph` package with either the `R-INLA` or `inlabru` (Bachl et al., 2019) interfaces of the `rSPDE` package (Bolin and Simas, 2023), as shown in the vignettes by Bolin et al. (2023b,c).

4 Numerical Experiments

To demonstrate the performance of the proposed approximation, we consider the interval, circle, and tadpole graphs shown in Figure 7. We examine these specific graphs because the corresponding covariance function of the solution u in each case is known, see Appendix I.

Using these three graphs, we consider a FEM mesh with step-size of $h = 1/1000$ and for the orders of the rational approximation, we consider $m = 1, 2, 3, 4, 5$. For the smoothness parameter α , we choose values ranging from 0.6 to 2.0. We further choose τ such that the marginal variance is close to 1 and set κ such that the practical correlation range ρ is fixed to 0.1, 0.5, 1, or 2. The approximation errors for the tadpole case and all possible combinations of parameters are shown in Figure 8. Similar illustrations for the interval and circle cases are shown in Appendix J.

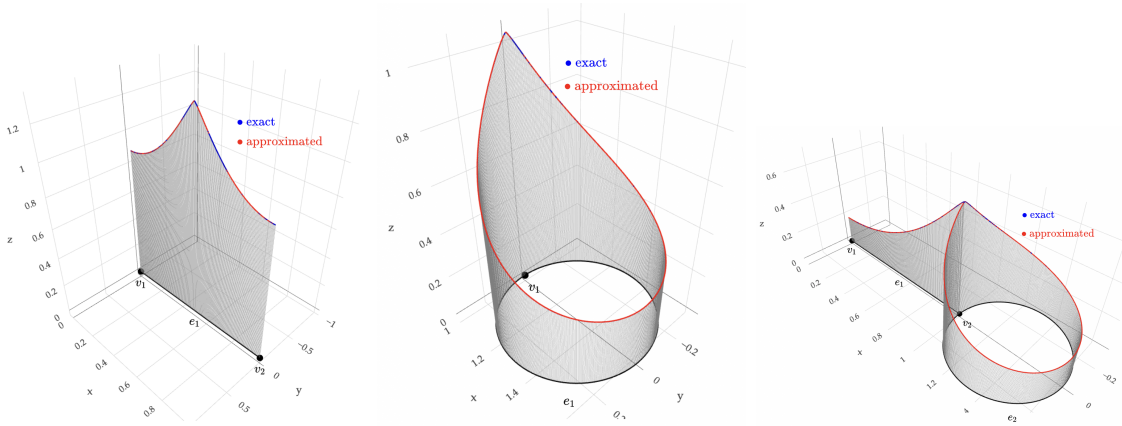


Figure 7: For each graph, exact (blue) and approximate (red) covariances $\varrho^\alpha(s_0, s)$ are shown for a fixed point s_0 . In all cases, the $h = 0.003$, $\alpha = 1.1$, $m = 4$, and $\rho = 1$.

Table 1: Observed rates of convergence for the covariance errors in Figure 9.

α	0.75	0.875	1	1.125	1.5
Theoretical rates	1	1.25	1.5	1.75	2
Interval graph	0.97	1.24	1.48	1.69	2.01
Circle graph	0.96	1.22	1.46	1.65	1.92
Tadpole graph	1.01	1.24	1.47	1.67	1.93

We observe that the error decreases fast in m and that the errors for different m collapse to a common point when $\alpha = 1$ and $\alpha = 2$, as there for these cases is no rational approximation and the only source of error is the FEM approximation. As ρ increases, numerical instabilities become present for large values of m , especially when $\alpha > 2$. Similar trends are observed for the interval and circle cases.

To verify that we indeed obtain the convergence rate $\min\{2\alpha - 1/2, 2\}$ as a function of h if we calibrate the order of the rational approximation according to (12), we consider $\rho = 0.5$, $\sigma = 1$, $\alpha = n/8$ for $n = 6, 7, 8, 9, 12$, compute the error for $h = 2^{-\ell}$ for $\ell = 4.5, 4.75, 5, 5.25, 5.5$. The empirical convergence rate is obtained by determining the slope r in the regression $\log \text{error} = c + r \log h$, where $\text{error} \approx \|\varrho - \varrho_{h,m}^\alpha\|_{L_2(\Gamma \times \Gamma)}$ is approximated as $\text{error}^2 = \mathbf{w}_{\text{ok}}^\top (\mathbf{\Sigma}_{\text{ok}} - A \mathbf{\Sigma}_h A^\top)^2 \mathbf{w}_{\text{ok}}$. Here, $\mathbf{\Sigma}_h$ is the covariance matrix of the true covariance evaluated on a fine mesh with mesh size $h_{\text{ok}} = 2^{-10}$, and $\mathbf{\Sigma}_{\text{ok}}$ is the exact covariance matrix on a mesh with $h = h_{\text{ok}}$. Further, A is a projector matrix with entries $\psi_j^h(s_i)$, ψ_j^h is the j th FEM basis function associated to the coarse mesh, s_i is the i th node location in the fine mesh, and \mathbf{w}_{ok} is a vector of weights $w_i = (\psi_i^{h_{\text{ok}}}, 1)_{L_2(\Gamma)}$. The results, shown in Figure 9 and Table 1 confirms that the empirical rates are close to the theoretical ones.

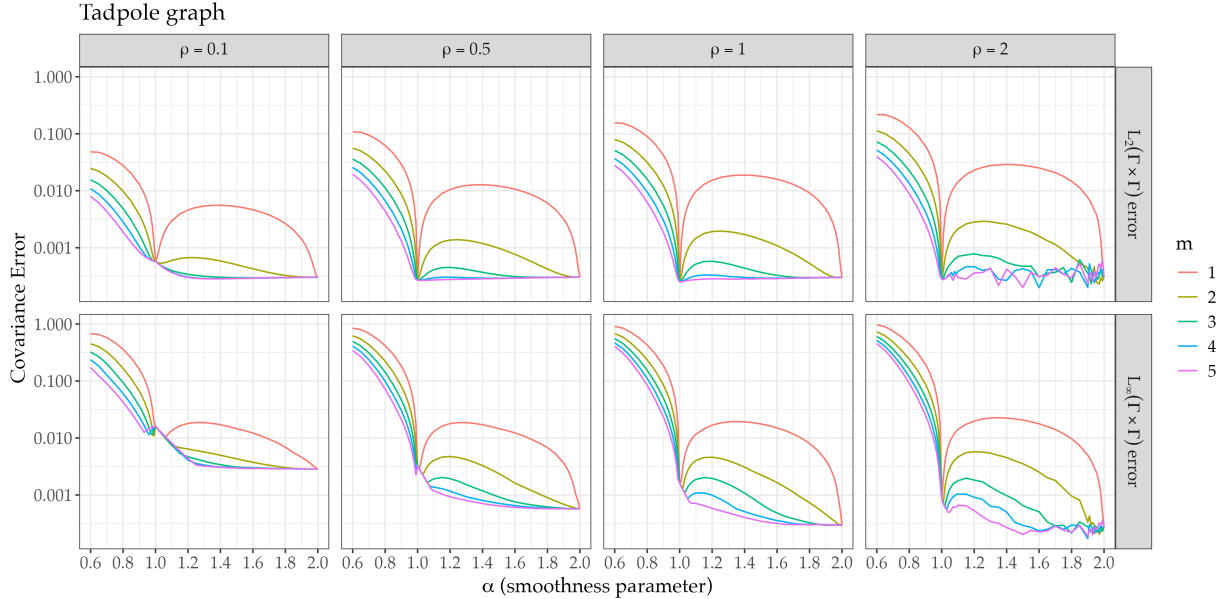


Figure 8: Covariance errors in the $L_2(\Gamma \times \Gamma)$ -norm (top) and supremum norm (bottom) on the tadpole graph for different practical correlation ranges ρ , smoothness α , and rational approximation orders m . In all cases, the FEM mesh has 3000 equally spaced nodes.

5 Application

5.1 The data

To illustrate the capabilities of the proposed method, we consider traffic speed data from the highway system in San Jose, California, obtained from the California Performance Measurement System database (Chen et al., 2001). The data set consists of 26 replicates, recorded by automatic sensors weekly on Mondays at 17:30, from January 2, 2017, to June 26, 2017. Each replicate contains $n = 325$ speed records (in mph), observed at different locations which are fixed across the replicates. Figure 10 shows speed records corresponding to the 14th replicate, observed on April 3, 2017. The highway network was obtained from OpenStreetMap (OpenStreetMap contributors, 2017) and, when converted to a metric graph object, consists of 691 vertices and 848 edges.

Borovitskiy et al. (2021) averaged this data across replicates and modeled the n observations using a graph Laplacian-based model restricted to the vertices. Bolin et al. (2023a) used a Whittle–Matérn field to model the same data. Here, we do not average the data across replicates. The first 13 replicates are used to construct covariates, while the remaining 13 are used for modeling. Eleven locations were removed beforehand, as their recorded values were constant across the first 13 replicates. Figures 11 and 12 display the mean and standardized logarithm of the standard deviation for these replicates, showing that the data is not stationary.

5.2 Constructing covariates with sufficient regularity

Identifying meaningful covariates for this data is challenging. One natural candidate is the speed limit, but available resources show it is the same for all roads. To derive a

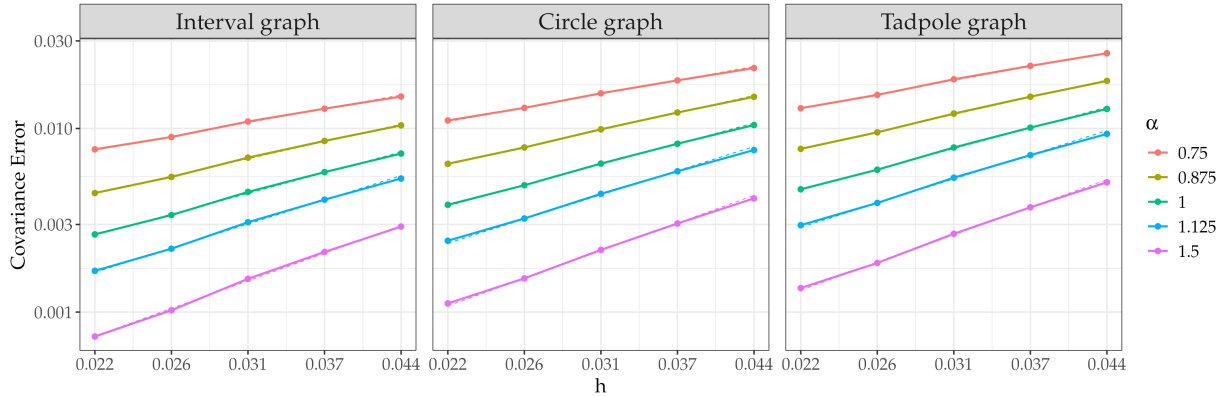


Figure 9: Observed covariance error for different values of α as functions of the mesh size h . The dashed lines show the theoretical rates for each case.

covariate for expected speed, use an approach similar to that in Section 2.6. Specifically, we calculate the average speed m_i at each observation location s_i , $i = 1, \dots, 314$, using the first 13 replicates. We then fit the model $m_i | u(\cdot) \sim N(\beta_0 + u(s_i), \sigma_\epsilon^2)$, where u is a Whittle–Matérn field with α estimated from the data. The covariate $\text{mean.cov}(s)$ is defined as the kriging predictor $\mathbb{E}(u(s) | m_1, \dots, m_{314})$ (see Figure 11).

Similarly, we construct a covariate for τ and κ in the non-stationary Whittle–Matérn field by fitting the model $\log \text{std}_i \sim N(\beta_0 + u(s_i), \sigma_\epsilon^2)$ to the standard deviations std_i of the data at the observation locations in the first 13 replicates. The covariate $\text{std.cov}(s)$ is then defined as the kriging predictor $\mathbb{E}(u(s) | \log \text{std}_1, \dots, \log \text{std}_{314})$ standardized by subtracting its mean and dividing by its standard deviation (see Figure 12). As we showed earlier, the regularity of τ in (1) is crucial for the regularity of the Gaussian field. A key advantage of this method for constructing the covariate is that if $\log \tau$ is modeled as $\log \tau(s) = \theta_1 + \theta_3 \cdot \text{std.cov}(s)$, then, by Propositions 5 and 6, τ satisfies the regularity conditions of Proposition 3.

5.3 The models for the data

We now model the second part of the data by assuming that the speed records y_i are observations of 13 independent replicates satisfying

$$y_i | u(\cdot) \sim N(\beta_0 + \beta_1 \text{mean.cov}(s_i) + u(s_i), \sigma_\epsilon^2), \quad i = 1, \dots, 314, \quad (13)$$

where $u(\cdot)$ is a Gaussian process on the highway network. We consider Whittle–Matérn fields with stationary parameters $\kappa, \tau > 0$ and Generalized Whittle–Matérn fields where τ and κ are non-stationary following log-regressions

$$\log \tau(s) = \theta_1 + \theta_3 \cdot \text{std.cov}(s) \quad \text{and} \quad \log \kappa(s) = \theta_2 + \theta_4 \cdot \text{std.cov}(s). \quad (14)$$

For each of the two classes of models, we consider three scenarios for the smoothness parameter: when (1) ν is fixed to 0.5 or (2) 1.5, and (3) ν is estimated from the data. Thus, in total we have six different models.

The models are fitted to the data using `MetricGraph` and `inlabru` (the code available at <https://github.com/leninrafaelrierasegura/GWMF>). The posterior means of the

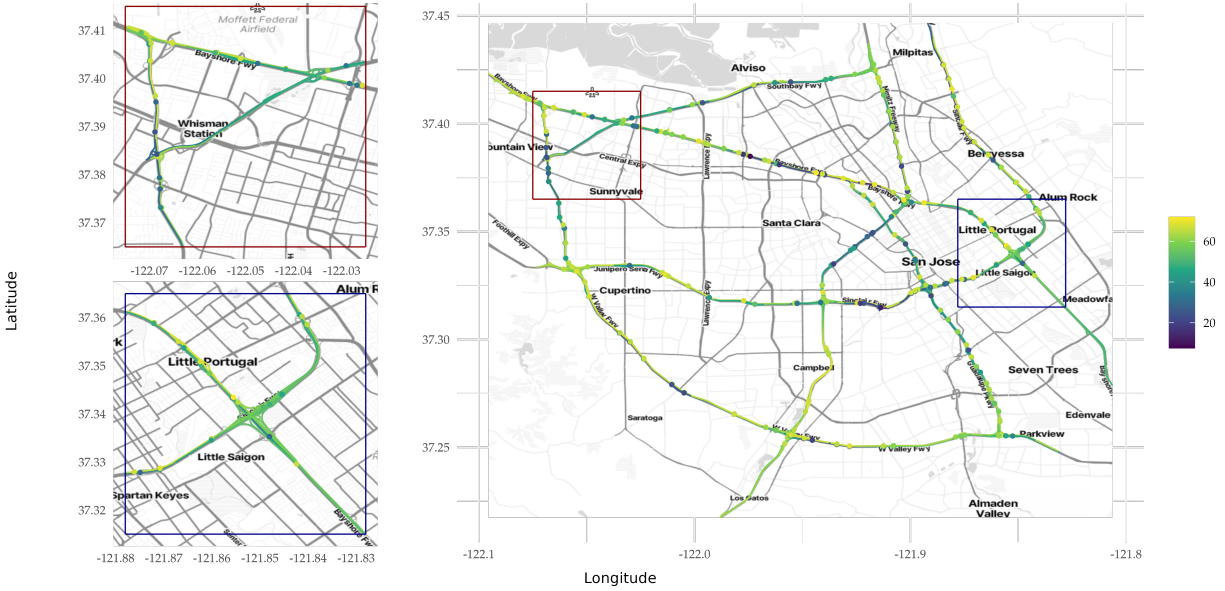


Figure 10: Speed observations (in mph) on the highway network of the city of San Jose in California, recorded on April 3, 2017. Points represent the observations, and the color on the edges represent the model prediction. The left panels show two zoomed-in areas.

Table 2: Posterior means of the parameters of stationary models.

ν	β_0	β_1	τ	κ	σ_e
0.5	-14.782	1.283	0.222	0.052	8.570
1.5	-16.501	1.316	0.331	0.256	8.788
est = 0.506	-14.778	1.282	0.223	0.055	8.569

parameter estimates can be seen in Tables 2 and 3. All estimates in both tables are significantly different from zero. From Table 2, we observe that the estimates for β_0 , β_1 , and σ_e are relatively stable regardless of the smoothness of the field, suggesting that the effect of the covariate and the residual variability of the model remain robust across different levels of spatial smoothness. The estimates for τ and κ are quite similar for the cases where $\nu = 0.5$ and ν is estimated. However, they differ significantly for the case $\nu = 1.5$, as the model needs to adjust to a smoother field. When $\nu = 1.5$, the spatial process becomes smoother, requiring a larger κ to reduce the spatial dependence range, allowing the correlation to decay more quickly over shorter distances. For the non-stationary models (Table 3), we also observe some consistency in the estimates of β_0 , β_1 , and σ_e , especially when $\nu = 0.5$ and ν is estimated. However, for the parameters θ_i , $i = 1, 2, 3, 4$ in (14), the estimates vary considerably between the three cases, suggesting that the parameters in (14) are sensitive to changes in ν .

5.4 Comparison using cross-validation

We compare the predictive performance of the six models using leave-group-out pseudo cross-validation (Liu and Rue, 2024), and specifically the strategy from Bolin et al. (2024), where predictions at each location are made by excluding the most informative observa-

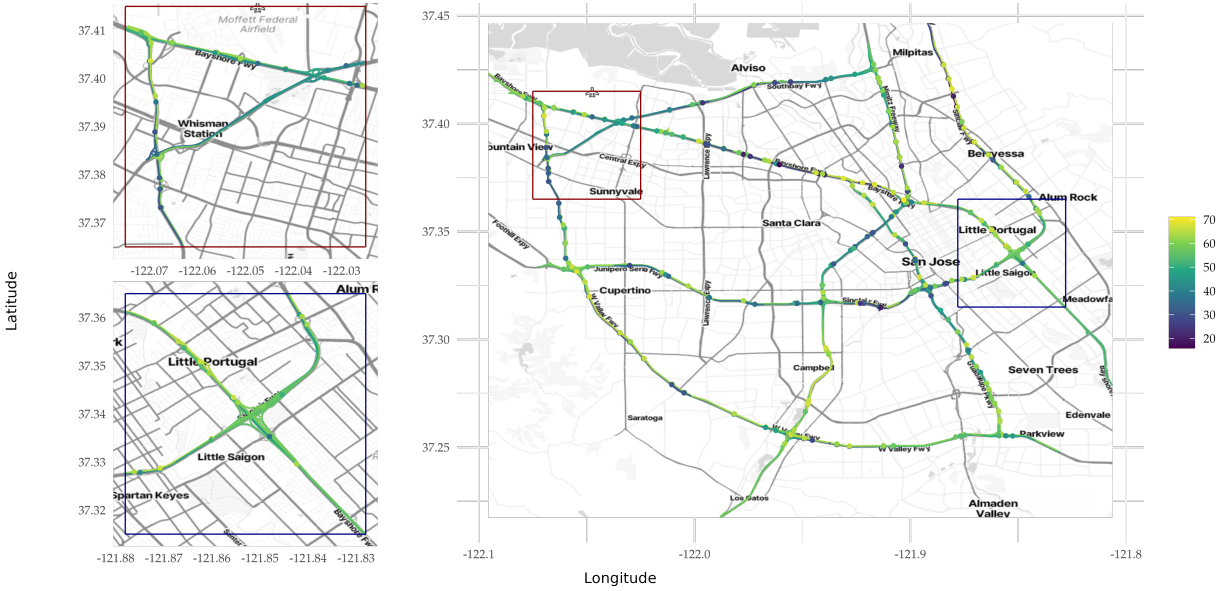


Figure 11: Average speeds of the first part of the data. Points represent the point value at each available location, and edges represent the mean.cov(s) covariate.

Table 3: Posterior means of the parameters of non-stationary models.

ν	β_0	β_1	θ_1	θ_2	θ_3	θ_4	σ_e
0.5	-4.732	1.130	-1.185	-5.252	-0.627	2.241	8.235
1.5	-4.472	1.126	-0.340	-2.028	-0.936	0.720	8.548
est = 0.526	-5.097	1.136	-1.176	-3.345	-0.589	0.564	8.272

tions—those within a specified radius R based on geodesic distance. By varying R , the model’s prediction accuracy is obtained as a function of R . We use the Mean Squared Errors (MSE) and the Negative Log-Score (NLS) (Good, 1952) as evaluation metrics.

Since the MSE and NLS are negatively oriented (less is better), Figure 13 shows that the non-stationary model outperforms its stationary counterpart, in both metrics and regardless of the distance and the value of ν (fixed or estimated). This highlights the benefit of allowing models with non-stationary features, providing an advantage over alternative proposals. Regarding the smoothness parameter ν , we observe that small values of ν produce better predictions, according to both metrics and regardless of the model class (stationary or not). For the stationary case, the estimated mean value of ν is 0.506, which is close to 0.5, thus explaining the proximity of the blue and red dot-dashed curves in both panels of Figure 13. For the non-stationary case, the estimated mean value of ν is 0.526, and a similar behavior is observed in this case. Because there is no improvement in the model’s performance when ν is estimated, we might as well prefer the model with $\nu = 0.5$ in this case. Reaching a conclusion like this is only possible because of our ability to estimate the smoothness parameter ν , which is evidence that allowing models with arbitrary smoothness is advantageous. Figure 10 shows the kriging predictor for the 14th replicate using the non-stationary model with $\nu = 0.5$, which is the best model in terms of predictive performance.

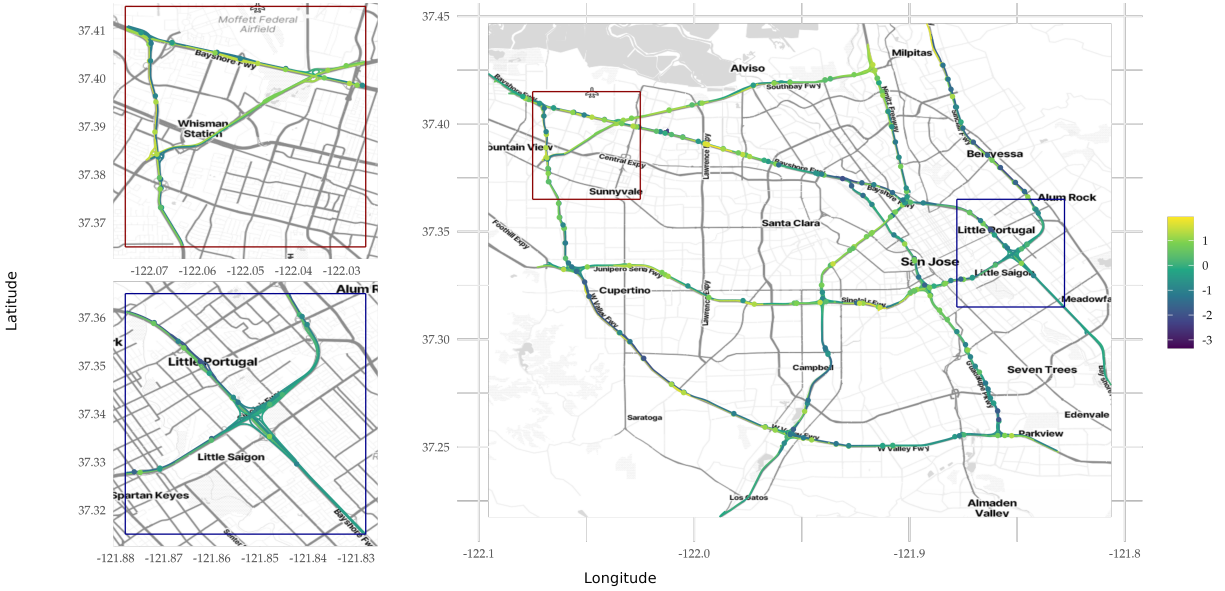


Figure 12: Standardized logarithm of the standard deviation for the first part of the data. Points show values at each location, and edges represent the $\text{std.cov}(s)$ covariate.

6 Conclusion

We have proposed a flexible class of Gaussian random fields for metric graphs, which allow for non-stationary covariance functions and general smoothness. By building upon a chain of results inspired by the SPDE approach in Euclidean domains, and by combining the FEM-based numerical approximation of Bolin et al. (2024) with the rational approximation of Bolin et al. (2024), we showed that the proposed class of models can be implemented in a computationally efficient way for general metric graphs, facilitating applications to large graphs and big data sets. The approach has been theoretically justified and numerical experiments verify the theoretical results. Further, the application presented demonstrated the advantages of the proposed approach for statistical modeling.

Future work could explore the extension of the proposed framework to spatio-temporal models. This could allow, for example, to understand how traffic flow and congestion in road networks evolve over time due to changing traffic conditions or to study the diffusion and temporal dynamics of pollutants in river networks for environmental monitoring. Additionally, the framework could be extended to log-Gaussian Cox processes (LGCPs), enabling the modeling of point patterns constrained to graph structures. Future work from a theoretical perspective involve extending the regularity results from Subsections 2.3 and 2.5, as well as proving strict positive definiteness for any $\alpha > 1/2$, under suitable assumptions on κ . While the restriction $\alpha \leq 2$ in Proposition 1 is unnecessary for the uniqueness proof, it is crucial for establishing strict positive definiteness and is required throughout the regularity results due to the limited smoothness of κ imposed by Assumption 1. These future extensions would likely rely on assumptions similar to those in Bolin et al. (2024b).

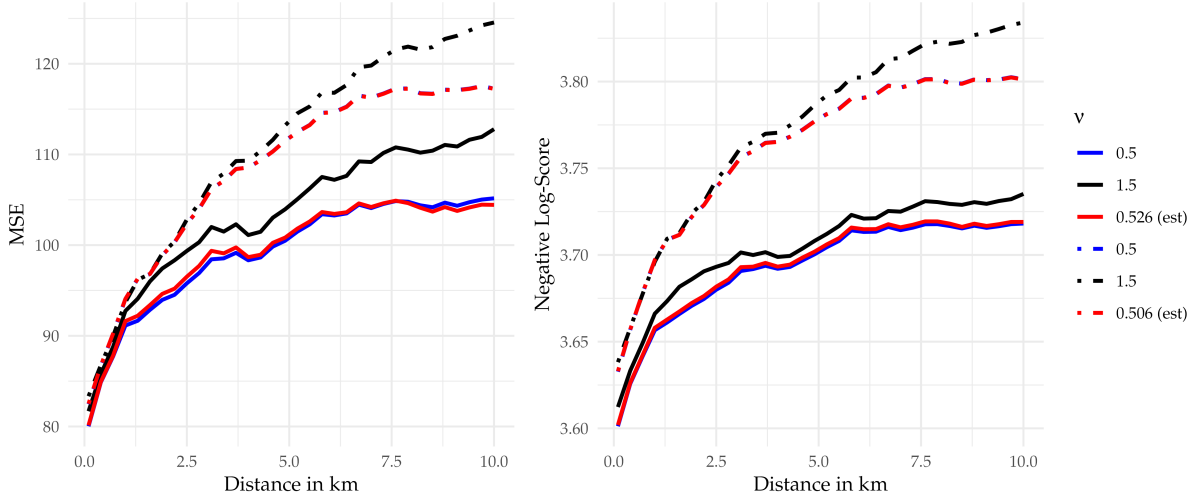


Figure 13: MSE and negative Log-Score as functions of distance (in km) for the stationary ($\cdot - \cdot$) and non-stationary (—) cases with $\nu = 0.5$, $\nu = 1.5$, and ν estimated (est).

A Additional notation

To support the technical details in the main text and the following appendices, we begin by introducing some additional notation. The Sobolev space $H^1(\Gamma)$ is defined as

$$H^1(\Gamma) = \{f \in C(\Gamma) : \|f\|_{H^1(\Gamma)}^2 < \infty\} = C(\Gamma) \cap \bigoplus_{e \in \mathcal{E}} H^1(e),$$

with the norm

$$\|f\|_{H^1(\Gamma)}^2 = \sum_{e \in \mathcal{E}} \|f_e\|_{H^1(e)}^2 = \sum_{e \in \mathcal{E}} \left(\int_e f_e'^2(s) ds + \int_e f_e^2(s) ds \right),$$

where, for each $e \in \mathcal{E}$, $H^1(e)$ is the standard Sobolev space of order 1 on $[0, \ell_e]$, and f_e' is the weak derivative of f_e , defined as the unique function in $L_2(e)$ satisfying

$$f_e(x) = f_e(0) + \int_0^x f_e'(s) ds \quad \text{for all } x \in [0, \ell_e]. \quad (15)$$

We also define the decoupled Sobolev spaces of integer order $k \geq 1$, by $\tilde{H}^k(\Gamma) = \bigoplus_{e \in \mathcal{E}} H^k(e)$, with norm $\|f\|_{\tilde{H}^k(\Gamma)}^2 = \sum_{e \in \mathcal{E}} \|f_e\|_{H^k(e)}^2$, where $H^k(e)$ is the standard Sobolev space of order k on the edge e . This space consists of functions in $L^2(e)$ whose weak derivatives up to order k also belong to $L^2(e)$. Higher-order weak derivatives are defined inductively, with the j -th derivative of a function f_e being the weak derivative of $f_e^{(j-1)}$, as given by (15). It follows that any $f_e \in H^1(e)$ is almost everywhere equal to a continuous function. Furthermore, if $f \in \tilde{H}^2(\Gamma)$, then for every $e \in \mathcal{E}$, f_e' can be identified with a continuous function.

To ensure continuity across Γ , we define the spaces $\tilde{H}_C^k(\Gamma) = \tilde{H}^k(\Gamma) \cap C(\Gamma)$. Note that $H^1(\Gamma) = \tilde{H}^1(\Gamma) \cap C(\Gamma) = \tilde{H}_C^1(\Gamma)$, so functions in $H^1(\Gamma)$ are guaranteed to be continuous, unlike functions in the decoupled Sobolev space $\tilde{H}^1(\Gamma)$. The space $K(\Gamma)$ is then defined as

the space of functions in $\tilde{H}_C^2(\Gamma)$ that satisfy the Kirchhoff vertex conditions. Specifically,

$$K(\Gamma) = \left\{ u \in \tilde{H}_C^2(\Gamma) \mid \forall v \in \mathcal{V}, \sum_{e \in \mathcal{E}_v} \partial_e u(v) = 0 \right\},$$

where ∂_e denotes the directional derivative along e , taken away from v . For $e = [0, \ell_e]$, if $v = 0$, then $\partial_e f(v) = f'_e(0)$, whereas if $v = \ell_e$, then $\partial_e f(v) = -f'_e(\ell_e)$. Further, $K(\Gamma)$ is well-defined since for functions $f \in \tilde{H}^2(\Gamma)$, f'_e can be identified with a continuous function, so the expression $\partial_e u(v)$ is meaningful.

Let $(E, \|\cdot\|_E)$ and $(F, \|\cdot\|_F)$ be two separable Hilbert spaces. We denote by $\mathcal{L}(E, F)$ the Banach space of linear bounded operators from E to F , equipped with the norm $\|\cdot\|_{\mathcal{L}(E, F)} = \sup_{\|x\|_E=1} \|\cdot x\|_F$. The space $\mathcal{L}_2(E, F)$ consists of Hilbert-Schmidt operators from E to F , with the Hilbert-Schmidt norm defined by

$$\|\cdot\|_{\mathcal{L}_2(E, F)}^2 = \sum_{j \in \mathbb{N}} \|\cdot e_j\|_F^2,$$

where $(e_j)_j$ is a complete orthonormal basis of E . For the special case $\mathcal{L}_2(E, E)$, we write $\mathcal{L}_2(E)$ for simplicity. If $E \subset F$ with continuous inclusion, i.e., there exists $C > 0$ such that $\|f\|_F \leq C\|f\|_E$ for all $f \in E$, we write $E \hookrightarrow F$. If $E \hookrightarrow F \hookrightarrow E$, we write $E \cong F$.

Let $(\Omega, \mathcal{F}, \mathbb{P})$ be a complete probability space. For a real-valued random variable Z , its expectation is given by $\mathbb{E}(Z) = \int_{\Omega} Z(\omega) d\mathbb{P}(\omega)$. The space $L_2(\Omega)$ denotes the Hilbert space of equivalence classes of real-valued random variables with finite second moments. For a separable Hilbert space $(E, \|\cdot\|_E)$, the space $L_2(\Omega; E)$ consists of E -valued Bochner-measurable random variables with finite second moments, equipped with the norm

$$\|u\|_{L_2(\Omega; E)}^2 = \int_{\Omega} \|u(\omega)\|_E^2 d\mathbb{P}(\omega).$$

If $E \subset F$, we denote the real interpolation space of order $s \in (0, 1)$ between F and E by $(F, E)_s$. The fractional Sobolev spaces are defined as follows:

$$H^s(\Gamma) := \begin{cases} (L_2(\Gamma), H^1(\Gamma))_s, & \text{for } 0 < s < 1, \\ (H^1(\Gamma), \tilde{H}_C^2(\Gamma))_{s-1}, & \text{for } 1 \leq s \leq 2, \end{cases}$$

$$\tilde{H}^s(\Gamma) := \begin{cases} (L_2(\Gamma), \tilde{H}^1(\Gamma))_s, & \text{for } 0 < s < 1, \\ (\tilde{H}^1(\Gamma), \tilde{H}^2(\Gamma))_{s-1}, & \text{for } 1 \leq s \leq 2. \end{cases}$$

The essential supremum and infimum of a function f over Γ are defined as:

$$\operatorname{ess\,sup}_{s \in \Gamma} |f(s)| := \inf\{M \geq 0 : \lambda(\{s \in \Gamma : |f(s)| > M\}) = 0\},$$

$$\operatorname{ess\,inf}_{s \in \Gamma} |f(s)| := \sup\{m \geq 0 : \lambda(\{s \in \Gamma : |f(s)| < m\}) = 0\},$$

where λ is the Lebesgue measure on Γ , given by $\lambda(A) = \sum_{e \in \mathcal{E}} \lambda_e(A \cap e)$, with λ_e being the Lebesgue measure on each edge e , identified with a compact interval.

The Gaussian linear space associated with a Gaussian random field u is defined as $H_u = \overline{\operatorname{span}\{u(s) : s \in \Gamma\}}$, where the closure is taken in $L_2(\Omega)$. If e is an edge and $f : e \rightarrow H_u$

is a function, we say that f is weakly differentiable at s in the $L_2(\Omega)$ sense if there exists $f'(s) \in H_u$ such that, for every $v \in H_u$ and every sequence $s_n \rightarrow s$ with $s_n \neq s$, we have

$$\mathbb{E} \left(v \frac{f(s_n) - f(s)}{s_n - s} \right) \rightarrow \mathbb{E}(wf'(s)).$$

Finally, the Cameron-Martin space (also known as the reproducing kernel Hilbert space) associated with u is defined as $\mathcal{H}_u = \{h(s) = \mathbb{E}(vu(s)) : s \in \Gamma, v \in H_u\}$.

B Preliminaries on Hölder spaces

In this section, we provide some general results on Hölder spaces which will be needed in what follows. The results are stated and proved for general metric spaces, as the proofs for metric graphs and general metric spaces are identical.

Let (X, \tilde{d}) be a metric space, and let $C(X)$ denote the space of real-valued continuous functions on X . For $\gamma \in (0, 1]$, the γ -Hölder seminorm is defined as

$$[f]_{C^{0,\gamma}(X)} = \sup_{s,s' \in X} \frac{|f(s) - f(s')|}{\tilde{d}(s, s')^\gamma},$$

where $f \in C(X)$. The space of functions $f \in C(X)$ with a finite seminorm $[f]_{C^{0,\gamma}(X)}$ is denoted by $C^{0,\gamma}(X)$. We equip the Hölder space $C^{0,\gamma}(X)$ with the norm

$$\|f\|_{C^{0,\gamma}(X)} = \|f\|_{C(X)} + [f]_{C^{0,\gamma}(X)},$$

for $f \in C^{0,\gamma}(X)$. A function $f \in C^{0,\gamma}(X)$ is referred to as γ -Hölder continuous.

We now state and prove some fundamental properties of the Hölder seminorm and, more generally, of Hölder spaces. All proofs are straightforward adaptations of those provided in Fiorenza (2017) for real-valued functions defined on subsets of \mathbb{R}^d , where $d \in \mathbb{N}$. We start by showing the relation between Hölder spaces with different exponents.

Throughout this section, (X, \tilde{d}) denotes a metric space.

Proposition 8. *Let $0 < \mu < \gamma \leq 1$ and define*

$$\delta = \text{diam } X = \sup_{x', x'' \in X} \tilde{d}(x', x'').$$

Then, for any $f \in C^{0,\gamma}(X)$, $[f]_{C^{0,\mu}(X)} \leq \delta^{\gamma-\mu} [f]_{C^{0,\gamma}(X)}$. In particular, if $\delta < \infty$ and f is γ -Hölder continuous, then f is also μ -Hölder continuous.

Proof. For any $x', x'' \in X$, we have

$$\begin{aligned} |f(x') - f(x'')| &\leq [f]_{C^{0,\gamma}(X)} \tilde{d}(x', x'')^\gamma = [f]_{C^{0,\gamma}(X)} \tilde{d}(x', x'')^{\gamma-\mu} \tilde{d}(x', x'')^\mu \\ &\leq [f]_{C^{0,\gamma}(X)} \delta^{\gamma-\mu} \tilde{d}(x', x'')^\mu. \end{aligned}$$

Thus, the inequality is satisfied and if $\delta < \infty$, then f is μ -Hölder continuous on X . \square

We will now show properties related to the sums, products and compositions of Hölder continuous functions. We start with the sum:

Proposition 9. *If f and g are γ -Hölder continuous on X , then their sum $f + g$ is also γ -Hölder continuous. Moreover, the Hölder seminorm satisfies*

$$[f + g]_{C^{0,\gamma}(X)} \leq [f]_{C^{0,\gamma}(X)} + [g]_{C^{0,\gamma}(X)}. \quad (16)$$

Proof. For any $x', x'' \in X$, we have

$$\begin{aligned} |(f + g)(x') - (f + g)(x'')| &\leq |f(x') - f(x'')| + |g(x') - g(x'')| \\ &\leq [f]_{C^{0,\gamma}(X)} \tilde{d}(x', x'')^\gamma + [g]_{C^{0,\gamma}(X)} \tilde{d}(x', x'')^\gamma \\ &= ([f]_{C^{0,\gamma}(X)} + [g]_{C^{0,\gamma}(X)}) \tilde{d}(x', x'')^\gamma. \end{aligned}$$

This shows that $f + g$ is γ -Hölder continuous, and that (16) holds. \square

Proposition 10. *If f and g are bounded and γ -Hölder continuous on X , then their product fg is also γ -Hölder continuous. Moreover, the Hölder seminorm satisfies*

$$[fg]_{C^{0,\gamma}(X)} \leq [f]_{C^{0,\gamma}(X)} \sup_{x \in X} |g(x)| + [g]_{C^{0,\gamma}(X)} \sup_{x \in X} |f(x)|. \quad (17)$$

Proof. For any $x', x'' \in X$, we have

$$\begin{aligned} |f(x')g(x') - f(x'')g(x'')| &= |f(x')g(x') - f(x'')g(x'') + f(x'')g(x') - f(x'')g(x'')| \\ &\leq |g(x')||f(x') - f(x'')| + |f(x'')||g(x') - g(x'')| \\ &\leq [f]_{C^{0,\gamma}(X)} \sup_{x \in X} |g(x)| \tilde{d}(x', x'')^\gamma + [g]_{C^{0,\gamma}(X)} \sup_{x \in X} |f(x)| \tilde{d}(x', x'')^\gamma \\ &= ([f]_{C^{0,\gamma}(X)} \sup_{x \in X} |g(x)| + [g]_{C^{0,\gamma}(X)} \sup_{x \in X} |f(x)|) \tilde{d}(x', x'')^\gamma. \end{aligned}$$

This shows that fg is γ -Hölder continuous, and that (17) holds. \square

Proposition 11. *If g is γ -Hölder continuous function on X such that $\inf_{x \in X} |g(x)| > 0$, then $1/g$ is also γ -Hölder continuous on X . Moreover, the Hölder seminorm satisfies*

$$\left[\frac{1}{g} \right]_{C^{0,\gamma}(X)} \leq \frac{[g]_{C^{0,\gamma}(X)}}{(\inf_{x \in X} |g(x)|)^2}.$$

Proof. For any $x', x'' \in X$, we have

$$\left| \frac{1}{g(x')} - \frac{1}{g(x'')} \right| = \left| \frac{1}{g(x')} - \frac{1}{g(x'')} \right| = \frac{|g(x') - g(x'')|}{|g(x')||g(x'')|} \leq \frac{[g]_{C^{0,\gamma}(X)}}{(\inf_{x \in X} |g(x)|)^2} \tilde{d}(x', x'')^\gamma,$$

which establishes the desired result. \square

Proposition 12. *Let f and g be γ -Hölder continuous functions on X . If g satisfies $\inf_{x \in X} |g(x)| > 0$, then f/g is also γ -Hölder continuous, and the Hölder seminorm satisfies*

$$\left[\frac{f}{g} \right]_{C^{0,\gamma}(X)} \leq \frac{[f]_{C^{0,\gamma}(X)} \sup_{x \in X} |g(x)| + [g]_{C^{0,\gamma}(X)} \sup_{x \in X} |f(x)|}{(\inf_{x \in X} |g(x)|)^2}.$$

Proof. The result follows directly from Proposition 10, with g replaced by $1/g$, and using Proposition 11. \square

Proposition 13. *If f and g are Hölder continuous functions, with f being γ -Hölder continuous on $Y = g(X)$ and g being μ -Hölder continuous on X , then the composition $f \circ g$ is $(\gamma\mu)$ -Hölder continuous. Moreover, the Hölder seminorm satisfies*

$$[f \circ g]_{C^{0,\gamma\mu}(X)} \leq [f]_{C^{0,\gamma}(Y)} ([g]_{C^{0,\mu}(X)})^\gamma. \quad (18)$$

Proof. For any $x', x'' \in X$, we have

$$\begin{aligned} |f(g(x')) - f(g(x''))| &\leq [f]_{C^{0,\gamma}(Y)} |g(x') - g(x'')|^\gamma \leq [f]_{C^{0,\gamma}(Y)} ([g]_{C^{0,\mu}(X)} \tilde{d}(x', x'')^\mu)^\gamma \\ &= [f]_{C^{0,\gamma}(Y)} ([g]_{C^{0,\mu}(X)})^\gamma \tilde{d}(x', x'')^{\gamma\mu}. \end{aligned}$$

Thus, $f \circ g$ is $(\gamma\mu)$ -Hölder continuous, and (18) holds. \square

C Uniqueness of the solution

We now proceed with a rigorous definition of the differential operator $L = \kappa^2 - \Delta_\Gamma$ under Assumption 1 from the main text, along with some of its fundamental properties. Recall that Δ_Γ is the Kirchhoff–Laplacian, acting on functions in $K(\Gamma)$. Specifically, Δ_Γ is defined on $K(\Gamma)$ and acts on a function $f \in K(\Gamma)$ in such a way that, for every $e \in \mathcal{E}$, we have $(\Delta_\Gamma f)|_e = f''_e$. Thus, the domain of Δ_Γ consists of continuous functions that are twice differentiable on each edge and satisfy the Kirchhoff vertex conditions specified in $K(\Gamma)$. These conditions enforce a sum-to-zero constraint on the directional derivatives at each vertex. In particular, this implies that the derivative is continuous at vertices of degree 2.

Under these assumptions, $L = \kappa^2 - \Delta_\Gamma$ is densely defined, selfadjoint, and positive definite with a compact inverse (Bolin et al., 2024). Consequently, it has a collection of eigenfunctions $(e_j)_j$, which form an orthonormal basis of $L_2(\Gamma)$, and corresponding eigenvalues $(\lambda_j)_j$. The fractional operator $L^{\alpha/2} : D(L^{\alpha/2}) \mapsto L_2(\Gamma)$ is then defined in the spectral sense as

$$\phi \mapsto L^{\alpha/2} \phi = \sum_{j \in \mathbb{N}} \lambda_j^{\alpha/2} (\phi, e_j)_{L_2(\Gamma)} e_j, \quad (19)$$

where $D(L^{\alpha/2}) = \dot{H}^\alpha = \{\phi \in L_2(\Gamma) : \|\phi\|_\alpha < \infty\}$ is a Hilbert space with inner product $(\phi, \psi)_\alpha = (L^{\alpha/2} \phi, L^{\alpha/2} \psi)_{L_2(\Gamma)}$ and induced norm $\|\phi\|_\alpha^2 = \|L^{\alpha/2} \phi\|_{L_2(\Gamma)}^2 = \sum_{j \in \mathbb{N}} \lambda_j^\alpha (\phi, e_j)_{L_2(\Gamma)}^2$.

Let, now, $M_g : L_2(\Gamma) \rightarrow L_2(\Gamma)$ be the multiplication operator by a function $g \in L_\infty(\Gamma)$ such that $\text{ess inf}_{s \in \Gamma} g(s) > 0$. Then, the operator M_g is self-adjoint and coercive, and hence has a unique inverse M_g^{-1} . We, thus, define a solution to equation (1) in the main text as a centered Gaussian random field u such that for all $h \in L_2(\Gamma)$,

$$(u, h)_{L_2(\Gamma)} = \mathcal{W}((M_\tau^{-1} L^{-\alpha/2})^* h) = \mathcal{W}(L^{-\alpha/2} (M_\tau^{-1} h)),$$

where T^* denotes the adjoint of a linear operator T and \mathcal{W} is Gaussian white noise on Γ introduced in the main text.

We are now in a position to prove the uniqueness part of Proposition 1:

Proof of Proposition 1 (uniqueness). Let $1/2 < \alpha$ and assume that Assumption 1 holds. Let, $\tau_\infty := \text{ess sup}_{s \in \Gamma} \tau(s) < \infty$, since $\tau \in L_\infty(\Gamma)$, and recall that $\tau_0 := \text{ess inf}_{s \in \Gamma} \tau(s) > 0$. Now, consider the following auxiliary problem:

$$(\kappa^2 - \Delta_\Gamma)^{\alpha/2} w = \mathcal{W}, \quad \text{on } \Gamma, \quad (20)$$

where \mathcal{W} is Gaussian white noise. This problem has a unique solution w by Bolin et al. (2024, Proposition 3.2). Define $\tilde{u} = \tau^{-1}w$, which is well-defined as $0 < \tau_0 \leq \tau \leq \tau_\infty < \infty$. Then, it follows that \tilde{u} is a solution to (1) in the main text. Conversely, in the same manner, if u is a solution to (1), then $\tilde{w} = \tau u$ is a solution to (20). This gives a one-to-one correspondence between solutions to (1) and (20). The uniqueness thus follows from the uniqueness of solutions to (20). \square

In order to prove positive definiteness statement of Proposition 1, we will need the following auxiliary result, which is an extension of Bolin et al. (2023a, Proposition 1).

Proposition 14. *Let $1/2 < \alpha \leq 2$, and let v be the solution to (20). Then, w has a strictly positive-definite covariance function.*

Proof. Let $\rho(\cdot, \cdot)$ be the covariance function of w . Now, observe that by Bogachev (1998, p. 44), the Cameron-Martin space associated to w is $\dot{H}^\alpha = D(L^{\alpha/2})$. Further, by Janson (1997, Corollary 8.16), the reproducing kernel Hilbert space associated to ρ is the Cameron-Martin space associated to w , that is, \dot{H}^α . We will now follow the proof of Bolin et al. (2023a, Proposition 1) and define the set

$$\mathcal{A}(\Gamma) = \langle 1 \rangle + D(\Gamma) + \mathcal{S}_c(\Gamma) = \{c + f + g : c \in \mathbb{R}, f \in D(\Gamma), g \in \mathcal{S}_c(\Gamma)\},$$

where $\langle 1 \rangle = \text{span}\{1\}$ is the space of constant functions on Γ , $D(\Gamma) = \bigoplus_{e \in E} C_c^\infty(e)$ is the space of functions with support in the union of the interiors of edges, whose restrictions to the edges are infinitely differentiable, and $\mathcal{S}_c(\Gamma)$ is a subspace defined as:

$$\mathcal{S}_c(\Gamma) = \{f \in C(\Gamma) : \exists v \in V, f \in \mathcal{S}_c(v, \Gamma) \cap \mathcal{N}(v, \Gamma)\},$$

where $\mathcal{S}_c(v, \Gamma)$ contains functions compactly supported within the star graph induced by the vertex v with the outer vertices removed, that is,

$$\mathcal{S}_c(v, \Gamma) = \{s \in \Gamma : s = (t, e), e \in \mathcal{E}_v, e = [0, \ell_e], t \in (0, \ell_e)\} \cup \{v\},$$

and

$$\mathcal{N}(v, \Gamma) = \left\{ f \in C(\Gamma) : \forall e, e' \in \mathcal{E}_v, f|_e \in C^\infty(e), \begin{array}{l} f_e^{(2k-1)}(v) = 0, \\ f_e^{(2k)}(v) = f_{e'}^{(2k)}(v), \forall k \in \mathbb{N} \end{array} \right\}.$$

Now, it follows immediately from Bolin et al. (2024, Theorem 4.1) that $\mathcal{A}(\Gamma) \subset \dot{H}^\alpha$, for $1/2 < \alpha \leq 2$. Furthermore, by Bolin et al. (2023a, Lemma 2), we have that $\mathcal{A}(\Gamma)$ is dense in $C(\Gamma)$ with respect to the $\|\cdot\|_{C(\Gamma)}$ norm. Therefore, \dot{H}^α is dense in $C(\Gamma)$ with respect to the $\|\cdot\|_{C(\Gamma)}$ norm, which, by Bolin et al. (2023a, Proposition 10 and Remark 4), implies that ρ is strictly positive-definite. \square

Proof of Proposition 1 (positive definiteness). The strict positive definiteness follows directly from the assumptions on τ and Proposition 14. Specifically, let w be the solution to (20), and note that $u = \tau^{-1}w$. The covariance function of u , denoted by $\varrho(\cdot, \cdot)$, is

$$\varrho(s, s') = \mathbb{E}[u(s)u(s')] = \mathbb{E}[\tau^{-1}(s)w(s)w(s')\tau^{-1}(s')] = \tau^{-1}(s)\rho(s, s')\tau^{-1}(s'), \quad s, s' \in \Gamma.$$

By Proposition 14, the function $\rho(\cdot, \cdot)$ is strictly positive-definite. This means that for any $n \in \mathbb{N}$, any nonzero vector $\mathbf{a} = (a_1, \dots, a_n) \in \mathbb{R}^n$, and any points $s_1, \dots, s_n \in \Gamma$, we have:

$$\sum_{i,j=1}^n a_i \rho(s_i, s_j) a_j > 0.$$

Since τ^{-1} is strictly positive by assumption, the vector $\mathbf{b} = (a_1 \tau^{-1}(s_1), \dots, a_n \tau^{-1}(s_n))$ is also nonzero. Thus, we can write:

$$0 < \sum_{i,j=1}^n b_i \rho(s_i, s_j) b_j = \sum_{i,j=1}^n a_i \tau^{-1}(s_i) \rho(s_i, s_j) \tau^{-1}(s_j) a_j = \sum_{i,j=1}^n a_i \varrho(s_i, s_j) a_j.$$

This shows that $\varrho(\cdot, \cdot)$ is strictly positive-definite, completing the proof. \square

D The role of $\tau(\cdot)$ in the regularity of the field

In this section, we provide proofs for Propositions 2 and 3. We begin with the proof of statement (i) of Proposition 2 and then proceed to prove statement (i) of Proposition 3. Throughout this section, we frequently utilize the auxiliary equation defined in (20).

Proof of statement (i) of Proposition 2. Let w be a solution to (20), and let $0 < \gamma < \tilde{\alpha}$ be as in the statement. Observe that $u = \tau^{-1}w$ is a solution to (1) in the main text. By Bolin et al. (2024, Lemma 4.6), w has a modification with γ -Hölder continuous sample paths on Γ . For the remaining of the proof we will assume we are considering such a modification. This implies that for every $e \in \mathcal{E}$, w_e has γ -Hölder continuous sample paths.

Under Assumption 1, note that τ^{-1} is bounded and bounded away from zero. Moreover, since w has continuous sample paths, these sample paths are bounded. Therefore, by Proposition 12, it follows that, for every $e \in \mathcal{E}$, the sample paths of $u_e = \tau^{-1}w_e$ are γ -Hölder continuous. \square

Proof of statement (i) of Proposition 3. By statement (i) of Proposition 2, u has a modification such that, for every $e \in \mathcal{E}$, u_e has γ -Hölder continuous sample paths. Let w be as in the proof of statement (i) of Proposition 2, so that w has a modification with γ -Hölder continuous sample paths on Γ . Since the sample paths of w are bounded, by Proposition 12, if $\tau \in C^{0,\gamma}(\Gamma)$ and τ satisfies Assumption 1, then the sample paths of $u = \tau^{-1}w$ are γ -Hölder continuous.

Now assume that $\tau \in C(\Gamma)$ and $\tau_e \in C^{0,\tilde{\alpha}}(e)$ for all $e \in \mathcal{E}$. Since w has a modification with γ -Hölder continuous sample paths, if τ is continuous on Γ , then $u = \tau^{-1}w$ has a modification with continuous sample paths.

Finally, let $1/2 < \alpha \leq 2$, and assume that $\tau_e \in C^{0,\tilde{\alpha}}(e)$ for all $e \in \mathcal{E}$, and that u has a modification with continuous sample paths. Let w be the solution to the auxiliary problem (20). Then, with probability 1, for every $v \in \mathcal{V}$, we have $u_e(v) = u_{e'}(v)$, for all $e, e' \in \mathcal{E}_v$. Substituting $u = \tau^{-1}w$, we thus have $\tau_e^{-1}(v)w_e(v) = \tau_{e'}^{-1}(v)w_{e'}(v)$, for all $e, e' \in \mathcal{E}_v$. Since w has almost surely continuous sample paths, it follows that $w_e(v) = w_{e'}(v)$, for all $e, e' \in \mathcal{E}_v$. Furthermore, by Proposition 14, w has a strictly positive-definite covariance function. Thus, for every $v \in \mathcal{V}$ and every $e \in \mathcal{E}_v$, we have $\mathbb{P}(w_e(v) \neq 0) = 1$. Consequently,

$$\tau_e^{-1}(v) = \tau_{e'}^{-1}(v), \quad \text{for all } e, e' \in \mathcal{E}_v. \quad (21)$$

Since τ_e is continuous on each edge $e \in \mathcal{E}$, equation (21) ensures the continuity of τ at all vertices $v \in \mathcal{V}$. Therefore, τ is continuous on Γ . \square

Our goal now is to prove statement (ii) from Proposition 2 and statement (ii) from Proposition 3. To such an end, we will need several auxiliary results. Let us first prove the following lemma, which is an extension of Bolin et al. (2024, Lemma 1).

Lemma D.1. *Fix $1/2 < \alpha \leq 2$ and let $\tilde{\alpha} = \min\{\alpha - 1/2, 1/2\}$. Further, let $\tilde{\Gamma} \subset \Gamma$ be a compact and connected metric graph contained in Γ . Assume that $T_\alpha : L_2(\Gamma) \rightarrow H^{\tilde{\alpha}}(\tilde{\Gamma})$ is a bounded linear operator. For a location $s \in \Gamma$, define $u_0 := \mathcal{W}(T_\alpha^* \delta_s)$, where δ_s is the Dirac measure concentrated at s and \mathcal{W} is Gaussian white noise on $L_2(\Gamma)$. Then,*

$$\mathbb{E} (|u_0(s) - u_0(s')|^2) \leq \|T_\alpha\|_{\mathcal{L}(L_2(\Gamma), C^{0,\tilde{\alpha}}(\tilde{\Gamma}))}^2 d(s, s')^{2\tilde{\alpha}}.$$

Thus, given $0 < \gamma < \tilde{\alpha}$, u_0 has a modification with γ -Hölder continuous sample paths.

Proof. The proof is essentially the same as the proof of Bolin et al. (2024a, Lemma 1). Therefore, we will only provide the parts in which the proof differs. Begin by observing that by Bolin et al. (2024a, Theorem 2), we have that $T_\alpha : L_2(\Gamma) \rightarrow H^{\tilde{\alpha}}(\tilde{\Gamma}) \hookrightarrow C^{0,\tilde{\alpha}}(\tilde{\Gamma})$. Thus, $T_\alpha : L_2(\Gamma) \rightarrow C^{0,\tilde{\alpha}}(\tilde{\Gamma})$ is a bounded operator. Let $T_\alpha^* : (C^{0,\tilde{\alpha}}(\tilde{\Gamma}))^* \rightarrow (L_2(\Gamma))^* = L_2(\Gamma)$ be the adjoint of T_α . Further, observe that $\delta_s \in (C^{0,\tilde{\alpha}}(\tilde{\Gamma}))^*$, which yields $T_\alpha^*(\delta_s) \in L_2(\Gamma)$. Therefore, $u_0 := \mathcal{W}(T_\alpha^*(\delta_s))$, is well-defined. The remaining proof is the same as the proof of Bolin et al. (2024, Lemma 1), with the replacement of $L^{-\alpha/2}$ by T_α . \square

The next lemma is an extension of Bolin et al. (2024a, Lemma 2) and shows that u_0 defined in Lemma D.1 is a centered Gaussian random field with covariance operator $T_\alpha T_\alpha^*$.

Lemma D.2. *Under the assumptions of Lemma D.1, fix $0 < \gamma < \tilde{\alpha}$ and let u_1 be any γ -Hölder continuous modification of u_0 . Then, for every $h \in L_2(\tilde{\Gamma})$, $(u_1, h)_{L_2(\tilde{\Gamma})} = \mathcal{W}(T_\alpha^* h)$.*

Proof. The proof follows the same steps as in Bolin et al. (2024a, Lemma 2), with the substitution of $L^{-\alpha/2}$ by T_α . All arguments remain identical under this replacement. \square

We now prove some additional results regarding the derivatives of the solution to the auxiliary problem (20), when $\alpha > 3/2$. To this end, we first recall some results from Bolin et al. (2024). The following lemma is a special case of Bolin et al. (2024, Lemma 5.5):

Lemma D.3. *For any $0 \leq s \leq 1$ and any edge $e \in \mathcal{E}$, the restriction operator $R_{e,s}$ is a bounded operator from $H^s(\Gamma)$ to $H^s(e)$ and from $\tilde{H}^s(e)$ to $\tilde{H}^s(\Gamma)$.*

To keep the notation simple, we will denote $R_{e,s}$ (i.e., the restriction operator from $H^s(\Gamma)$ to $H^s(e)$) by R_e . The next lemma is a special case of Bolin et al. (2024, Lemma 5.4) when $\Gamma = e$:

Lemma D.4. *Let $1 < s < 2$. Then, for any $e \in \mathcal{E}$, with the identification $e = [0, \ell_e]$, the derivative operator D such that $(Df_e)(x) = f'_e(x)$, for $f_e \in H^s(e)$, is a bounded operator from $H^s(e)$ to $H^{s-1}(e)$.*

The following results are novel, even in the context of standard Whittle–Matérn fields, where κ is constant in the auxiliary problem.

Proposition 15. *Let $\alpha > 3/2$ and let w be the solution to (20). Then, for any $e \in \mathcal{E}$, and $t, t' \in [0, \ell_e]$,*

$$\mathbb{E} (|w'_e(t) - w'_e(t')|^2) \leq \|DR_e L^{-\alpha/2}\|_{\mathcal{L}(L_2(\Gamma), C^{0, \alpha-3/2}(e))} |t - t'|^{2\alpha-3}, \quad t, t' \in e. \quad (22)$$

Further, for any $0 < \gamma < \alpha - 3/2$, w'_e has a modification with γ -Hölder continuous sample paths.

Proof. First, let $T_\alpha = DR_e L^{-\alpha/2}$. Then, T_α is a bounded operator from $L_2(\Gamma)$ to $C^{0, \alpha-3/2}(e)$. Indeed, $L^{-\alpha/2}$ is a bounded operator from $L_2(\Gamma)$ to \dot{H}^α . By Bolin et al. (2024, Theorem 4.1), we have that $\dot{H}^\alpha \hookrightarrow \tilde{H}^\alpha(\Gamma)$. Now, by Lemma D.3, $R_e L^{-\alpha/2}$ is a bounded operator from $L_2(\Gamma)$ to $H^\alpha(e)$. Next, by Lemma D.4, D is a bounded operator from $H^\alpha(e)$ to $H^{\alpha-1}(e)$. Finally, by the Sobolev embedding (Bolin et al., 2024a, Corollary 6), we have $H^{\alpha-1}(e) \hookrightarrow C^{0, \alpha-3/2}(e)$. Therefore, T_α is a bounded operator from $L_2(\Gamma)$ to $C^{0, \alpha-3/2}(e)$.

Let $u_0 := \mathcal{W}(T_\alpha^* \delta_s)$, where δ_s is the Dirac measure concentrated at s . By Lemma D.1, for any $0 < \gamma < \alpha - 3/2$, u_0 has a modification with γ -Hölder continuous sample paths. Next, by Lemma D.2, u_0 is a centered Gaussian random field with covariance operator $T_\alpha T_\alpha^* = DR_e L^{-\alpha} (DR_e)^*$.

Now, let w be the solution to (20), so that w has covariance operator $L^{-\alpha}$ and by Bolin et al. (2024, Theorem 4.4), the sample paths of w belong to $H^1(\Gamma)$, so that the sample paths of w are weakly differentiable. Then, $w'_e = DR_e w$, the derivative of w restricted to e , is a centered Gaussian random field with covariance operator $DR_e L^{-\alpha} (DR_e)^*$. Therefore, by the above, w'_e and u_0 have the same finite-dimensional distributions, which implies (22) and also implies that w'_e has a modification with γ -Hölder continuous sample paths. \square

We are now in a position to prove the statement (ii) from Proposition 2.

Proof of statement (ii) of Proposition 2. Let w be the solution to (20). Since $\alpha > 3/2$, it follows from Bolin et al. (2024, Theorem 4.4) that the sample paths of w belong to $H^1(\Gamma)$. Furthermore, by Proposition 15, w'_e has a modification with γ -Hölder continuous sample paths for any $0 < \gamma < \alpha - 3/2$. Fix $0 < \gamma < \alpha - 3/2$ and let w be a modification of w such that for every $e \in \mathcal{E}$, w'_e has γ -Hölder continuous sample paths. Since the sample paths of w belong to $H^1(\Gamma)$, it follows from (15) that for every $t \in e$,

$$w_e(t) = \int_0^t w'_e(s) ds + w_e(0).$$

Since, with probability 1, w'_e is continuous, it follows that w_e is continuously differentiable. Finally, since w'_e has γ -Hölder continuous sample paths, it follows that the sample paths of w_e belong to $C^{1, \gamma}(e)$.

Finally, if $\tau_e \in C^{1, \gamma}(e)$, and $\tau \geq \tau_0 > 0$, then $u_e = \tau_e^{-1} w_e$ is continuously differentiable. Further, $u'_e = \tau_e^{-1} w'_e - \tau_e^{-2} w_e \tau'_e$, which is γ -Hölder continuous by Propositions 8, 9, 10 and 12. Therefore, since e is compact, u has a modification such that for all $e \in \mathcal{E}$, u_e has sample paths belonging to $C^{1, \gamma}(e)$. \square

Before proving the final case, statement (ii) of Proposition 3, we need the following lemma. This lemma shows that the reciprocal of a function satisfying the Kirchhoff vertex conditions, as well as the product of functions satisfying the Kirchhoff vertex conditions, also satisfy the Kirchhoff vertex conditions. Here, $C^1(e)$ denotes the set of functions that are continuously differentiable on e .

Lemma D.5. *Let $f, g, h \in C(\Gamma)$ be functions such that, for every $e \in \mathcal{E}$, $f_e, g_e, h_e \in C^1(e)$, and they satisfy the Kirchhoff vertex conditions (2) from the main text. Then, the product fg also satisfies the Kirchhoff vertex conditions. Moreover, if h satisfies $h(s) \geq h_0$ for all $s \in \Gamma$, where $h_0 > 0$, then h^{-1} also satisfies the Kirchhoff vertex conditions.*

Proof. Let f, g, h be as in the statement. Then, h^{-1} and fg are continuous. Further,

$$\sum_{e \in \mathcal{E}_v} \partial_e h^{-1}(v) = - \sum_{e \in \mathcal{E}_v} (h_e^{-1}(v))^2 \partial_e h(v) = - \frac{1}{(h(v))^2} \sum_{e \in \mathcal{E}_v} \partial_e h(v) = 0,$$

where in the next to last equality we used the continuity of h . Therefore, h^{-1} satisfies the Kirchhoff vertex conditions. Similarly, by using the continuity of f and g ,

$$\begin{aligned} \sum_{e \in \mathcal{E}_v} \partial_e (fg)(v) &= \sum_{e \in \mathcal{E}_v} g_e(v) \partial_e f(v) + \sum_{e \in \mathcal{E}_v} f_e(v) \partial_e g(v) \\ &= g(v) \sum_{e \in \mathcal{E}_v} \partial_e f(v) + f(v) \sum_{e \in \mathcal{E}_v} \partial_e g(v) = 0. \end{aligned}$$

Therefore, fg satisfies the Kirchhoff vertex conditions. \square

Next, we present a novel result showing that for $\alpha > 3/2$, the solutions to (20) satisfy the Kirchhoff vertex conditions. This result improves upon Bolin et al. (2024a, Proposition 11), where it was established only for $\alpha \geq 2$ and limited to standard Whittle–Matérn fields, i.e., the case where κ is constant.

Proposition 16. *Let $\alpha > 3/2$, fix some $0 < \gamma < \alpha - 3/2$, and let w be the solution to (20). By Proposition 15, w admits a modification such that, for every $e \in \mathcal{E}$, the sample paths of w_e belong to $C^{1,\gamma}(e)$. This modification of w satisfies the Kirchhoff vertex conditions (2); specifically, the sample paths of w are continuous, and for all $v \in \mathcal{V}$, $\sum_{e \in \mathcal{E}_v} \partial_e w(v) = 0$.*

Proof. The continuity of w follows from Bolin et al. (2024, Theorem 4.4). Furthermore, by Bogachev (1998, p. 44), the Cameron-Martin space associated with w is given by \dot{H}^α . By Bolin et al. (2024, Theorem 4.1), we also have $\dot{H}^\alpha \cong \tilde{H}^\alpha \cap C(\Gamma) \cap K_\alpha(\Gamma)$, where

$$K_\alpha(\Gamma) = \left\{ f \in \tilde{H}^\alpha(\Gamma) : \forall v \in \mathcal{V}, \sum_{e \in \mathcal{E}_v} \partial_e f(v) = 0 \right\}. \quad (23)$$

Therefore, by the definition of the Cameron-Martin space, along with the above identification, we have $\{h(s) = \mathbb{E}(w(s)g) : s \in \Gamma, g \in H_w\} = \tilde{H}^\alpha \cap C(\Gamma) \cap K_\alpha(\Gamma)$. From Lemma D.3, for every $h \in \tilde{H}^\alpha$, $h|_e = R_e(h) \in H^\alpha(e)$. By the same arguments as in the proof of Proposition 15, we have $h_e \in C^{1,\gamma}(e)$.

Given any $g \in H_w$, define $h(s) = \mathbb{E}(w(s)g)$. For every edge $e \in \mathcal{E}$, $h_e = h|_e$ is continuously differentiable on $[0, \ell_e]$. Hence, for any $t \in [0, \ell_e]$ and any sequence $t_n \rightarrow t$, $t_n \in [0, \ell_e]$ with $t_n \neq t$, the sequence

$$\frac{w_e(t_n) - w_e(t)}{t_n - t}$$

is weakly Cauchy in H_w . Since H_w is a Hilbert space, it is weakly sequentially complete. Thus, there exists $w'_e(t) \in H_w$ such that

$$\frac{w_e(t_n) - w_e(t)}{t_n - t} \xrightarrow{w} w'_e(t),$$

where \xrightarrow{w} denotes weak convergence in H_w . Since the sample paths of w_e belong to $C^{1,\gamma}(e)$, the limit $w'_e(t)$ coincides with the classical derivative of w_e .

Because $h_e(t) = \mathbb{E}(w_e(t)g)$ is differentiable, the limit $w'_e(t)$ does not depend on the choice of the sequence $t_n \rightarrow t$. Moreover, the weak convergence implies $h'_e(t) = \mathbb{E}(w'_e(t)g)$, where we take lateral derivatives if t lies on the boundary of $[0, \ell_e]$. This proves the existence of the weak derivative in the $L_2(\Omega)$ -sense.

Since $h \in \mathcal{H}_w$, we have $h \in K_\alpha(\Gamma)$. Therefore, for every $v \in \mathcal{V}$,

$$0 = \sum_{e \in \mathcal{E}_v} \partial_e h(v) = \sum_{e \in \mathcal{E}_v} \partial_e \mathbb{E}(w_e(v)g) = \sum_{e \in \mathcal{E}_v} \mathbb{E}(\partial_e w_e(v)g) = \mathbb{E}\left[\left(\sum_{e \in \mathcal{E}_v} \partial_e w_e(v)\right)g\right],$$

where, for $e = [0, \ell_e]$, $\partial_e w_e(v) = w'_e(0)$ if $v = 0$, and $\partial_e w_e(v) = -w'_e(\ell_e)$ if $v = \ell_e$.

Finally, take $g = \sum_{e \in \mathcal{E}_v} \partial_e w_e(v)$, which belongs to H_w , since, as shown above, $w'_e \in H_w$ for every $e \in \mathcal{E}$. Then, $\mathbb{E}\left[\left(\sum_{e \in \mathcal{E}_v} \partial_e w_e(v)\right)^2\right] = 0$, which implies $\sum_{e \in \mathcal{E}_v} \partial_e w_e(v) = 0$, completing the proof. \square

We are now in a position to prove the final statement of Proposition 3.

Proof of statement (ii) of Proposition 3. Let w be the solution to (20) and let w_e be the restriction of w to e . By Proposition 16, w satisfies the Kirchhoff vertex conditions (2). The result thus follows from the fact that $u = \tau^{-1}w$ together with Lemma D.5. \square

E Proof of Proposition 4

First, let w be the solution to (20) and observe that by Bolin et al. (2024, Lemma 4.6),

$$\|w(s) - w(s')\|_{L_2(\Omega)} = \sqrt{\mathbb{E}(|w(s) - w(s')|^2)} \leq \|L^{-\alpha/2}\|_{\mathcal{L}(L_2(\Gamma), C^{0,\tilde{\alpha}}(\Gamma))} d(s, s')^{\tilde{\alpha}}.$$

Thus, we have that

$$\left| \|w(s)\|_{L_2(\Omega)} - \|w(s')\|_{L_2(\Omega)} \right| \leq \|w(s) - w(s')\|_{L_2(\Omega)} \leq \|L^{-\alpha/2}\|_{\mathcal{L}(L_2(\Gamma), C^{0,\tilde{\alpha}}(\Gamma))} d(s, s')^{\tilde{\alpha}}.$$

Now, note that $\|w(s)\|_{L_2(\Omega)} = \sqrt{\mathbb{E}(w(s)^2)} = \sigma_\kappa(s)$. Therefore, this shows that $\sigma_\kappa \in C^{0,\tilde{\alpha}}(\Gamma)$. This proves part of statement (i). Further, this shows that σ_κ is continuous in the compact set Γ . By Proposition 14, we have that for every $s \in \Gamma$, $\sigma_\kappa(s) > 0$. Thus, there exists $\sigma_{min} > 0$ such that for every $s \in \Gamma$, $\sigma_\kappa(s) \geq \sigma_{min} > 0$, which shows that Assumption 1 holds. The proof of statement (i) is concluded by applying statement (i) of Proposition 3.

Let us now prove statement (ii). To this end, let $\alpha > 3/2$ and start by observing that for every $e \in \mathcal{E}$, and every $t \in e$, we have that

$$\tau'_e(t) = \frac{\sigma_0^{-1}}{2\sigma_{\kappa,e}(t)} (\partial_1 \rho_e(t, t) + \partial_2 \rho_e(t, t)),$$

where $\rho(\cdot, \cdot)$ is the covariance function of w , $\sigma_{\kappa, e} = \sigma_\kappa|_e$, ρ_e is the restriction of ρ to $e \times e$, ∂_j stands for the partial derivative with respect to the j -th argument. Further, by symmetry, we have that $\partial_1 \rho_e(t, t) = \partial_2 \rho_e(t, t)$. Thus, we have that

$$\tau'_e(t) = \frac{\sigma_0^{-1} \partial_1 \rho_e(t, t)}{\sigma_{\kappa, e}(t)}.$$

Now, from the first part of the proof, $\sigma_\kappa \in C^{0, \tilde{\alpha}}(\Gamma)$. Thus, to show that $\tau_e \in C^{1, \alpha-3/2}(e)$, it suffices to show that the function $t \mapsto \partial_1 \rho_e(t, t)$ is $(\alpha - 3/2)$ -Hölder continuous.

To such an end, observe that by the same arguments as in the proof of Proposition 16, we have that for every $e \in \mathcal{E}$ and every $t \in e$, $\partial_1 \rho_e(t, t) = \mathbb{E}(w'_e(t)w_e(t))$, so that for $t, t' \in e$, we have that, by Cauchy-Schwarz, Proposition 15 and (Bolin et al., 2024, Lemma 4.6), there exists $C_e > 0$, that does not depend on t, t' , such that

$$\begin{aligned} |\partial_1 \rho_e(t, t) - \partial_1 \rho_e(t, t')| &= |\mathbb{E}(w'_e(t)w_e(t)) - \mathbb{E}(w'_e(t')w_e(t'))| \\ &= |\mathbb{E}(w'_e(t)(w_e(t) - w_e(t'))) + \mathbb{E}(w_e(t')(w'_e(t) - w'_e(t')))| \\ &\leq |\mathbb{E}(w'_e(t)(w_e(t) - w_e(t')))| + |\mathbb{E}(w_e(t')(w'_e(t) - w'_e(t')))| \\ &\leq \sqrt{\mathbb{E}(w'_e(t)^2)} \sqrt{\mathbb{E}((w_e(t) - w_e(t'))^2)} \\ &\quad + \sqrt{\mathbb{E}(w_e(t')^2)} \sqrt{\mathbb{E}((w'_e(t) - w'_e(t'))^2)} \\ &\leq C_e \sqrt{\mathbb{E}(w'_e(t)^2)} |t - t'|^{1/2} + C_e \sqrt{\mathbb{E}(w_e(t')^2)} |t - t'|^{\alpha-3/2} \\ &= C_e \sqrt{\mathbb{E}(w'_e(t)^2)} |t - t'|^{1/2} + C_e \sigma_{\kappa, e}(t') |t - t'|^{\alpha-3/2}. \end{aligned}$$

Now, observe that $\sigma_\kappa(\cdot)$ is continuous in the compact set Γ , so that it is bounded. Let $C_\kappa > 0$ be such that $\sigma_\kappa(s) \leq C_\kappa$ for every $s \in \Gamma$. Further, let $\widehat{\sigma}_\kappa(t) = \sqrt{\mathbb{E}(w'_e(t)^2)}$, and observe that by Proposition 15 and the same arguments as in the first part of the proof, we have that $\widehat{\sigma}_\kappa \in C^{0, \alpha-3/2}(\Gamma)$, and since Γ is compact, it is bounded. By changing C_κ if necessary, we may assume that $\widehat{\sigma}_\kappa(t) \leq C_\kappa$ for every $t \in \Gamma$. Thus, we have that

$$|\partial_1 \rho_e(t, t) - \partial_1 \rho_e(t, t')| \leq C_e C_\kappa (|t - t'|^{1/2} + |t - t'|^{\alpha-3/2}) \leq C_e C_\kappa (\ell_e^{2-\alpha} + 1) |t - t'|^{\alpha-3/2}.$$

Therefore, for every $e \in \mathcal{E}$, we have that $t \mapsto \partial_1 \rho_e(t, t)$ is $(\alpha - 3/2)$ -Hölder continuous. Hence, in view of the previous results, this shows that $\tau_e \in C^{1, \alpha-3/2}(e)$.

Finally, it remains to be shown that τ satisfies the Kirchhoff conditions. By the first part of the proof, τ is continuous. Now, for every $v \in \mathcal{V}$, we have, by continuity of σ_κ , that

$$\sum_{e \in \mathcal{E}_v} \partial_e \tau(v) = \sum_{e \in \mathcal{E}_v} \frac{\sigma_0^{-1}}{\sigma_{\kappa, e}(v)} \partial_1 \rho_e(v, v) = \sum_{e \in \mathcal{E}_v} \frac{\sigma_0^{-1}}{\sigma_{\kappa, e}(v)} \partial_1 \rho_e(v, v) = \frac{\sigma_0^{-1}}{\sigma_\kappa(v)} \sum_{e \in \mathcal{E}_v} \partial_1 \rho_e(v, v).$$

Thus, to conclude the proof, we need to show that $\sum_{e \in \mathcal{E}_v} \partial_1 \rho_e(v, v) = 0$. In fact, we have that by continuity of w and Proposition 16, that

$$\sum_{e \in \mathcal{E}_v} \partial_1 \rho_e(v, v) = \sum_{e \in \mathcal{E}_v} \mathbb{E}(w'_e(v)w_e(v)) = \mathbb{E}\left(\sum_{e \in \mathcal{E}_v} w'_e(v)w_e(v)\right) = \mathbb{E}\left(w(v) \sum_{e \in \mathcal{E}_v} w'_e(v)\right) = 0.$$

This concludes the proof. \square

F Proofs of Propositions 5 and 6

Proof of Proposition 5. First, let $h : \Gamma \rightarrow \mathbb{R}$ be defined as

$$h(s) = \theta_0 + \sum_{j=1}^m \theta_j g_j(s), \quad s \in \Gamma.$$

By Proposition 9 together with the fact that $g_1, \dots, g_m \in C^{0,\gamma}(\Gamma)$, we have $h \in C^{0,\gamma}(\Gamma)$.

Now, observe that since Γ is a compact metric space and h is continuous, there exists $M > 0$ such that $|h(s)| \leq M$ for all $s \in \Gamma$. Now, observe that, by the mean-value theorem, $t \mapsto \exp(t)$ is Lipschitz (that is, 1-Hölder continuous) on the interval $[-M, M]$. Therefore, by using the fact that $h \in C^{0,\gamma}(\Gamma)$ and $\exp(\cdot)$ is Lipschitz in $[-M, M] \supset h(\Gamma)$, we can apply Proposition 13 to obtain that

$$s \mapsto \exp(h(s)) = \exp\left(\theta_0 + \sum_{j=1}^m \theta_j g_j(s)\right)$$

is γ -Hölder continuous, that is, $\tau \in C^{0,\gamma}(\Gamma)$. This proves the first part of the proposition.

Now, suppose that for every $e \in \mathcal{E}$, $g_{1,e}, \dots, g_{m,e} \in C^{1,\gamma}(e)$, and that each g_j satisfies the Kirchhoff conditions, that is, equation (2) in the main text. Then, since for every $e \in \mathcal{E}$, the functions $\exp(\cdot)$ and $h(\cdot)$ are continuously differentiable on e , the function $\tau(\cdot) = \exp(h(\cdot))$ is continuously differentiable on e .

Now, observe that, by the chain rule, $\tau'_e(s) = \exp(h_e(s))h'_e(s)$, where $h_e(\cdot)$ is the restriction of $h(\cdot)$ to e . Further, since $h_e(\cdot)$ is continuously differentiable on e and e is compact, we have that $h'_e(s)$ is bounded on e . Therefore, there exists $M > 0$ such that $|\tau'_e(s)| \leq M$ for all $s \in e$, and by the mean-value theorem, $\tau_e(\cdot) = \exp(h_e(\cdot))$ is Lipschitz on e (or, 1-Hölder continuous on e). In particular, by Proposition 8, $\tau_e(\cdot) \in C^{0,\gamma}(e)$. Furthermore, since $g_{1,e}, \dots, g_{m,e} \in C^{1,\gamma}(e)$, we have that $g'_{1,e}, \dots, g'_{m,e} \in C^{0,\gamma}(e)$. Hence, $h'_e \in C^{0,\gamma}(e)$. Therefore, by Proposition 10, $\tau'_e(\cdot) = \exp(h_e(\cdot))h'_e(\cdot)$ is γ -Hölder continuous, that is, $\tau'_e \in C^{0,\gamma}(e)$, which implies that $\tau_e \in C^{1,\gamma}(e)$.

It remains to be shown that $\tau(\cdot)$ satisfies the Kirchhoff conditions. The continuity follows from the first part of the proof. Thus, since $\tau(\cdot) = \exp(h(\cdot))$ is continuous, we have that for every $v \in \mathcal{V}$,

$$\begin{aligned} \sum_{e \in \mathcal{E}_v} \partial_e \tau(v) &= \sum_{e \in \mathcal{E}_v} \partial_e \exp(h(v)) = \sum_{e \in \mathcal{E}_v} \exp(h(v)) \partial_e h(v) = \exp(h(v)) \sum_{e \in \mathcal{E}_v} \partial_e h(v) \\ &= \exp(h(v)) \sum_{e \in \mathcal{E}_v} \sum_{j=1}^m \theta_j \partial_e g_j(v) = \exp(h(v)) \sum_{j=1}^m \theta_j \sum_{e \in \mathcal{E}_v} \partial_e g_j(v) = 0. \end{aligned}$$

This concludes the proof. \square

We will now prove Proposition 6. But first, let us prove an auxiliary result that tells us that the kriging predictor belongs to the Cameron-Martin space associated to the solutions w to equation (6) in the main text. First, recall, from Section A, that the Cameron-Martin space associated to w is $\mathcal{H}_w = \{h(s) = \mathbb{E}(vu(s)) : s \in \Gamma, v \in H_w\}$, where $H_w = \text{span}\{w(s) : s \in \Gamma\}$ is the Gaussian space associated to w .

Lemma F.1. *Under the same assumptions, and using the same notation, as in Proposition 6, the centered kriging predictor $\tilde{z}(\cdot) := z(\cdot) - \beta_0$ belongs to \mathcal{H}_w , where w is the solution to equation (6) in the main text.*

Proof. First, let $\rho(\cdot, \cdot)$ denote the covariance function of w . By Proposition 14, $\rho(\cdot, \cdot)$ is strictly positive definite. Define $\Sigma_n = (\rho(s_i, s_j))_{i,j=1}^n$. The kriging predictor $z(\cdot)$ is given by

$$z(s) = \beta_0 + \mathbf{c}_n(s)^\top \tilde{\Sigma}_n^{-1} (\mathbf{z} - \beta_0), \quad (24)$$

where $\mathbf{z} = (z_1, \dots, z_n)$, $\mathbf{c}_n(s) = (\rho(s, s_1), \dots, \rho(s, s_n))^\top$ for all $s \in \Gamma$. For direct observations, $\tilde{\Sigma}_n = \Sigma_n$, while for noisy observations following (5) in the main text, $\tilde{\Sigma}_n = \Sigma_n + \sigma_e^2 \mathbf{I}_n$, where \mathbf{I}_n is the $n \times n$ identity matrix. The matrix $\tilde{\Sigma}_n^{-1}$ exists because $\rho(\cdot, \cdot)$ is strictly positive definite.

Now, observe that the expression for $\mathbf{c}_n(\cdot)$ allows us to write

$$\tilde{z}(s) = \mathbf{c}_n(s)^\top \tilde{\Sigma}_n^{-1} (\mathbf{z} - \beta_0) = \sum_{j=1}^n \alpha_{j,n} \rho(s, s_j),$$

where $\alpha_{j,n} \in \mathbb{R}$ do not depend on s . Therefore, by taking $v_j = w(s_j)$, we have that

$$\rho(\cdot, s_j) = \mathbb{E}(w(s_j)w(\cdot)) = \mathbb{E}(v_j w(\cdot)) \in \mathcal{H}_w,$$

for all $j = 1, \dots, n$. The proof is completed by observing that $\tilde{z}(\cdot)$ is a linear combination of elements in \mathcal{H}_w , and that \mathcal{H}_w is a vector space. \square

We are now in a position to prove Proposition 6:

Proof of Proposition 6. Begin by observing that, by Lemma F.1, $\tilde{z}(\cdot) \in \mathcal{H}_w$. Further, as in the proof of Proposition 16, we have that \mathcal{H}_w is given by \dot{H}^α . By Bolin et al. (2024, Theorem 4.1), we have that $\dot{H}^\alpha \hookrightarrow C^{0,\tilde{\alpha}}(\Gamma)$, where $\tilde{\alpha} = \min\{\alpha - 1/2, 1/2\}$. This proves that $\tilde{z}(\cdot) \in C^{0,\tilde{\alpha}}(\Gamma)$. Further, since the constant function equal to β_0 also belongs to $C^{0,\tilde{\alpha}}(\Gamma)$, we have that $z(\cdot) \in C^{0,\tilde{\alpha}}(\Gamma)$. By Proposition 8, and the fact that Γ is compact, we have that for any $0 < \gamma \leq \tilde{\alpha}$, $z(\cdot) \in C^{0,\gamma}(\Gamma)$. This proves the first claim.

Let us now prove the second claim. To such an end, let $\alpha > 3/2$, and observe that by Bolin et al. (2024, Theorem 4.1), we have that $\dot{H}^\alpha \subset \tilde{H}^\alpha(\Gamma) \subset \tilde{H}^1(\Gamma)$. In particular, $z \in \tilde{H}^1(\Gamma)$, so that for every $e \in \mathcal{E}$, with the identification $e = [0, \ell_e]$, we have

$$z_e(x) = z_e(0) + \int_0^x z'_e(t) dt,$$

where $z'_e(\cdot)$ is the weak derivative of $z_e(\cdot)$. Now, let D be the derivative operator acting on $H^\alpha(e)$, and R_e the restriction operator from $H^\alpha(\Gamma)$ to $H^\alpha(e)$. Then, we have by Lemmas D.3 and D.4 that $DR_e : \tilde{H}^\alpha(\Gamma) \rightarrow H^{\alpha-1}(e)$, so that

$$z'_e(\cdot) = DR_e z(\cdot) \in H^{\alpha-1}(e).$$

On the other hand, observe that, by the Sobolev embedding (Bolin et al., 2024a, Corollary 6), we have $H^{\alpha-1}(e) \hookrightarrow C^{0,\alpha-3/2}(e)$. Thus, $z'_e(\cdot) \in C^{0,\alpha-3/2}(e)$. In particular, for every $e \in \mathcal{E}$, we have $z_e(\cdot) \in C^{1,\alpha-3/2}(e)$. By Proposition 8, and the fact that Γ is compact, we have that

for any $0 < \gamma \leq \alpha - 1/2$, $z_e(\cdot) \in C^{1,\gamma}(e)$. To conclude the proof, note that by Bolin et al. (2024, Theorem 4.1) and the fact that $\alpha > 3/2$, we have that $\dot{H}^\alpha \subset K_\alpha(\Gamma)$, where $K_\alpha(\Gamma)$ is given in (23). Thus, since $z(\cdot) \in \dot{H}^\alpha$, it follows that $z(\cdot) \in K_\alpha(\Gamma)$, which in turn implies that $z(\cdot)$ satisfies the Kirchhoff conditions given by (2) in the main text. This concludes the proof. \square

G Finite element approximation

To construct the finite element discretization, each edge $e \in \mathcal{E}$ is subdivided into $n_e \geq 2$ regular segments of length h_e , which are delimited by the nodes

$$0 = x_0^e < x_1^e < \dots < x_{n_e-1}^e < x_{n_e}^e = \ell_e.$$

For each $j = 1, \dots, n_e - 1$, we consider the following standard hat basis functions

$$\varphi_j^e(x) = \begin{cases} 1 - \frac{|x_j^e - x|}{h_e}, & \text{if } x_{j-1}^e \leq x \leq x_{j+1}^e, \\ 0, & \text{otherwise.} \end{cases}$$

For each $e \in \mathcal{E}$, the set of hat functions $\{\varphi_1^e, \dots, \varphi_{n_e-1}^e\}$ is a basis for the space

$$V_{h_e} = \left\{ w \in H_0^1(e) \mid \forall j = 0, 1, \dots, n_e - 1 : w|_{[x_j^e, x_{j+1}^e]} \in \mathbb{P}^1 \right\},$$

where \mathbb{P}^1 is the space of linear functions on $[0, \ell_e]$. For each vertex $v \in \mathcal{V}$, we define

$$\mathcal{N}_v = \left\{ \bigcup_{e \in \{e \in \mathcal{E}_v : v = x_0^e\}} [v, x_1^e] \right\} \cup \left\{ \bigcup_{e \in \{e \in \mathcal{E}_v : v = x_{n_e}^e\}} [x_{n_e-1}^e, v] \right\},$$

which is a star-shaped set with center at v and rays made of the segments contiguous to v . On \mathcal{N}_v , we define the hat functions as

$$\phi_v(x) = \begin{cases} 1 - \frac{|x_v^e - x|}{h_e}, & \text{if } x \in \mathcal{N}_v \cap e \text{ and } e \in \mathcal{E}_v, \\ 0, & \text{otherwise,} \end{cases}$$

where x_v^e is either x_0^e or $x_{n_e}^e$ depending on the edge direction and its parameterization. See Arioli and Benzi (2018) for more details.

Figure 6 in the main text provides an illustration of the system of basis functions $\{\varphi_j^e, \phi_v\}$ (solid gray lines) on $\Gamma = (\mathcal{V}, \mathcal{E})$, where $\mathcal{E} = \{e_1, \dots, e_8\}$ and $\mathcal{V} = \{v_1, \dots, v_7\}$. Note that for all $e_i \in \mathcal{E}$, $n_{e_i} = 3$ and $h_{e_i} = 1/3$. In particular, for edge e_7 , observe that the three regular segments are delimited by the nodes $v_6 = x_0^{e_7} < x_1^{e_7} < x_2^{e_7} < x_3^{e_7} = v_7$. Corresponding to node $x_1^{e_7}$, we have plotted the basis function $\varphi_1^{e_7}$ in blue. The set \mathcal{N}_{v_2} is depicted in green and its corresponding basis function ϕ_{v_2} is shown in red.

Recall, from Subsection 3.2 of the main text the definition of the discretized operator L_h . This operator L_h is positive definite and has a collection of eigenvalues $(\lambda_{j,h})_{j=1}^{N_h}$ that

can be arranged as $0 < \lambda_{1,h} \leq \dots \leq \lambda_{N_h,h}$ and satisfy $\lambda_j \leq \lambda_{j,h}, j \in \mathbb{N}$ (Bolin et al., 2024, Sec. 6.3). The corresponding eigenfunctions, $(e_{j,h})_j$, are orthonormal in $L_2(\Gamma)$.

Having introduced the system of basis functions $\{\varphi_j^e, \phi_v\}$ (in the main text, we do not distinguish between them and refer to them jointly as $\{\psi_j\}_{j=1}^{N_h}$), we can now define the finite element space $V_h \subset H^1(\Gamma)$ as $V_h = (\bigoplus_{e \in \mathcal{E}} V_{h_e}) \bigoplus V_v$, where $V_v = \text{span}(\{\phi_v : v \in \mathcal{V}\})$ and $\dim(V_h)$ is given by $N_h = |\mathcal{V}| + \sum_{e \in \mathcal{E}} n_e$.

In what follows, $P_h : L_2(\Gamma) \rightarrow V_h$ represents the $L_2(\Gamma)$ -orthogonal projection onto V_h , h denotes $\max_{e \in \mathcal{E}} h_e$, and the expression $A \lesssim_{\alpha_1, \dots, \alpha_k} B$ indicates that $A \leq CB$ for some constant $C = C(\alpha_1, \dots, \alpha_k)$, where the parameters $\alpha_1, \dots, \alpha_k$ represent given data.

Proposition 17. *Let Assumption 1 hold, let $\alpha > 1/2$, and ϱ^α be the covariance function of the solution to the auxiliary problem (20). Let, now, ϱ_h^α be the covariance function of the solution to the discretized auxiliary problem $L_h^{\alpha/2} w_h = \mathcal{W}_h$, where is Gaussian white noise defined on V_h , introduced in the main text. Then,*

$$\|\varrho^\alpha - \varrho_h^\alpha\|_{L_2(\Gamma \times \Gamma)} \lesssim_{\sigma, \alpha, \kappa, \Gamma} h^\sigma \quad (25)$$

where $\sigma < \min\{2\alpha - 1/2, 2\}$.

A detailed proof of this result can be found in Bolin et al. (2024, Thm. 6.9). Proposition 17 provides an approximation of ϱ^α via ϱ_h^α , which essentially translates to approximating its corresponding covariance operator $L^{-\alpha}$ with $L_h^{-\alpha}$. This is a consequence of the relationship between the norm of a Hilbert-Schmidt integral operator and its kernel.

H Proof of Proposition 7

By the relationship of a kernel operator and its kernel function, together with the triangle inequality, we have that

$$\begin{aligned} \|\varrho^\alpha - \varrho_{h,m}^\alpha\|_{L_2(\Gamma \times \Gamma)} &= \|M_{\tau-1} L^{-\alpha} M_{\tau-1} - M_{\tau-1} r_m(L_h^{-1}) P_h M_{\tau-1}\|_{\mathcal{L}_2(L_2(\Gamma))} \\ &\leq \|M_{\tau-1} L_h^{-\alpha} P_h M_{\tau-1} - M_{\tau-1} r_m(L_h^{-1}) P_h M_{\tau-1}\|_{\mathcal{L}_2(L_2(\Gamma))} \\ &\quad + \|M_{\tau-1} L^{-\alpha} M_{\tau-1} - M_{\tau-1} L_h^{-\alpha} P_h M_{\tau-1}\|_{\mathcal{L}_2(L_2(\Gamma))} \end{aligned}$$

We can estimate each of the above terms as follows.

$$\begin{aligned} &\|M_{\tau-1} L_h^{-\alpha} P_h M_{\tau-1} - M_{\tau-1} r_m(L_h^{-1}) P_h M_{\tau-1}\|_{\mathcal{L}_2(L_2(\Gamma))} \\ &= \|M_{\tau-1} (L_h^{-\alpha} P_h - r_m(L_h^{-1}) P_h) M_{\tau-1}\|_{\mathcal{L}_2(L_2(\Gamma))} \\ &\leq \|M_{\tau-1}\|_{\mathcal{L}(L_2(\Gamma))} \| (L_h^{-\alpha} P_h - r_m(L_h^{-1}) P_h) M_{\tau-1} \|_{\mathcal{L}_2(L_2(\Gamma))} \\ &\leq \|M_{\tau-1}\|_{\mathcal{L}(L_2(\Gamma))}^2 \|L_h^{-\alpha} P_h - r_m(L_h^{-1}) P_h\|_{\mathcal{L}_2(L_2(\Gamma))} \\ &\leq \|\tau^{-1}\|_{L^\infty(\Gamma)}^2 \|L_h^{-\alpha} P_h - r_m(L_h^{-1}) P_h\|_{\mathcal{L}_2(L_2(\Gamma))} \\ &\|M_{\tau-1} L^{-\alpha} M_{\tau-1} - M_{\tau-1} L_h^{-\alpha} P_h M_{\tau-1}\|_{\mathcal{L}_2(L_2(\Gamma))} = \|M_{\tau-1} (L^{-\alpha} - L_h^{-\alpha} P_h) M_{\tau-1}\|_{\mathcal{L}_2(L_2(\Gamma))} \\ &\leq \|M_{\tau-1}\|_{\mathcal{L}(L_2(\Gamma))} \| (L^{-\alpha} - L_h^{-\alpha} P_h) M_{\tau-1} \|_{\mathcal{L}_2(L_2(\Gamma))} \\ &\leq \|M_{\tau-1}\|_{\mathcal{L}(L_2(\Gamma))}^2 \|L^{-\alpha} - L_h^{-\alpha} P_h\|_{\mathcal{L}_2(L_2(\Gamma))} \\ &\leq \|\tau^{-1}\|_{L^\infty(\Gamma)}^2 \|L^{-\alpha} - L_h^{-\alpha} P_h\|_{\mathcal{L}_2(L_2(\Gamma))} \end{aligned}$$

Therefore,

$$\begin{aligned} \|\varrho^\alpha - \varrho_{h,m}^\alpha\|_{L_2(\Gamma \times \Gamma)} &\leq \|\tau^{-1}\|_{L^\infty(\Gamma)}^2 \|L_h^{-\alpha} P_h - r_m(L_h^{-1}) P_h\|_{\mathcal{L}_2(L_2(\Gamma))} \\ &\quad + \|\tau^{-1}\|_{L^\infty(\Gamma)}^2 \|L^{-\alpha} - L_h^{-\alpha} P_h\|_{\mathcal{L}_2(L_2(\Gamma))}. \end{aligned}$$

From Proposition 17, we have that

$$\|L^{-\alpha} - L_h^{-\alpha} P_h\|_{\mathcal{L}_2(L_2(\Gamma))} \lesssim_{\sigma, \alpha, \kappa, \Gamma} h^\sigma. \quad (26)$$

This means that we only need to upper bound the term $\|L_h^{-\alpha} P_h - r_m(L_h^{-1}) P_h\|_{\mathcal{L}_2(L_2(\Gamma))}$. Recall that the eigenvalues of L_h are $0 < \lambda_{1,h} \leq \dots \leq \lambda_{N_h,h}$ with corresponding eigenfunctions $(e_{j,h})_j$, which are orthonormal in $L_2(\Gamma)$. Since $\lambda_j \leq \lambda_{j,h}$, $j \in \mathbb{N}$, we have that

$$0 < \frac{1}{\lambda_{N_h,h}} \leq \dots \leq \frac{1}{\lambda_{1,h}} \leq \frac{1}{\lambda_1}.$$

and therefore $J_h := [\lambda_{N_h,h}^{-1}, \lambda_{1,h}^{-1}] \subset [0, \lambda_1^{-1}] =: J$. Normalizing L , we get that $J_h \subset J \subset [0, 1]$. Let $f(x) = x^\alpha$ and $\hat{f}(x) = x^{\{\alpha\}}$. Since $\alpha = \lfloor \alpha \rfloor + \{\alpha\}$, we have that $f(x) = x^{\lfloor \alpha \rfloor} \hat{f}(x)$. Let $\hat{r}_m(x) = \frac{p(x)}{q(x)}$ be the best L_∞ -approximation of $\hat{f}(x)$ on J_h . Define $r_m(x) = x^{\lfloor \alpha \rfloor} \hat{r}_m(x)$.

Recall that $r_m(L_h^{-1}) = L_h^{-\lfloor \alpha \rfloor} p(L_h^{-1}) q(L_h^{-1})^{-1}$. Now

$$\begin{aligned} \|L_h^{-\alpha} P_h - r_m(L_h^{-1}) P_h\|_{\mathcal{L}_2(L_2(\Gamma))}^2 &= \sum_{j=1}^{N_h} \|L_h^{-\alpha} e_{j,h} - r_m(L_h^{-1}) e_{j,h}\|_{L_2(\Gamma)}^2 \\ &= \sum_{j=1}^{N_h} \|\lambda_{j,h}^{-\alpha} e_{j,h} - r_m(\lambda_{j,h}^{-1}) e_{j,h}\|_{L_2(\Gamma)}^2 \\ &= \sum_{j=1}^{N_h} (\lambda_{j,h}^{-\alpha} - r_m(\lambda_{j,h}^{-1}))^2 \|e_{j,h}\|_{L_2(\Gamma)}^2 \\ &= \sum_{j=1}^{N_h} (\lambda_{j,h}^{-\alpha} - r_m(\lambda_{j,h}^{-1}))^2 \leq \sum_{j=1}^{N_h} \max |\lambda_{j,h}^{-\alpha} - r_m(\lambda_{j,h}^{-1})|^2 \\ &= N_h \max_{1 \leq j \leq N_h} |\lambda_{j,h}^{-\alpha} - r_m(\lambda_{j,h}^{-1})|^2. \end{aligned} \quad (27)$$

Note that $x^{\lfloor \alpha \rfloor} \leq 1$ on $J_h \subset [0, 1]$ because $\lfloor \alpha \rfloor > 0$. Note also that $f(x) = x^\alpha \leq x^{\{\alpha\}} = \hat{f}(x)$ on $[0, 1]$. Hence,

$$\max_{1 \leq j \leq N_h} |(\lambda_{j,h}^{-1})^\alpha - r_m(\lambda_{j,h}^{-1})| \leq \sup_{x \in J_h} |f(x) - r_m(x)| \leq \sup_{x \in [0,1]} |\hat{f}(x) - \hat{r}_m(x)|. \quad (28)$$

From (Stahl, 2003, Thm. 1), we have that

$$\sup_{x \in [0,1]} |\hat{f}(x) - \hat{r}_m(x)| \lesssim e^{-2\pi \sqrt{\{\alpha\}m}}. \quad (29)$$

Combining (27), (28), and (29), we obtain that

$$\|L_h^{-\alpha} P_h - r_m(L_h^{-1}) P_h\|_{\mathcal{L}_2(L_2(\Gamma))} \lesssim N_h^{1/2} e^{-2\pi \sqrt{\{\alpha\}m}}.$$

Using that $N_h \lesssim h^{-1}$, $\|L_h^{-\alpha} P_h - r_m(L_h^{-1}) P_h\|_{\mathcal{L}_2(L_2(\Gamma))} \lesssim h^{-1/2} e^{-2\pi\sqrt{\{\alpha\}m}}$. Since this source of error only occurs when we employ the rational approximation,

$$\|L_h^{-\alpha} P_h - r_m(L_h^{-1}) P_h\|_{\mathcal{L}_2(L_2(\Gamma))} \lesssim 1_{\alpha \notin \mathbb{N}} h^{-1/2} e^{-2\pi\sqrt{\{\alpha\}m}}. \quad (30)$$

Combining (26) and (30), we obtain the desired result.

$$\begin{aligned} \|\varrho^\alpha - \varrho_{h,m}^\alpha\|_{L_2(\Gamma \times \Gamma)} &\lesssim_{\sigma, \alpha, \kappa, \Gamma} \|\tau^{-1}\|_{L^\infty(\Gamma)}^2 \left(h^\sigma + 1_{\alpha \notin \mathbb{N}} \cdot h^{-1/2} e^{-2\pi\sqrt{\{\alpha\}m}} \right) \\ &\lesssim_{\sigma, \alpha, \kappa, \tau, \Gamma} h^\sigma + 1_{\alpha \notin \mathbb{N}} \cdot h^{-1/2} e^{-2\pi\sqrt{\{\alpha\}m}}. \end{aligned}$$

□

I Covariance functions

For the interval and circle graph, the covariance function of the Whittle–Matérn field can be written in terms of the folded Matérn covariance function (Khristenko et al., 2019). Let

$$C(h) = \frac{\sigma^2}{2^{\nu-1}\Gamma(\nu)} (\kappa h)^\nu K_\nu(\kappa h), \quad h \geq 0,$$

be the Matérn covariance function, where $\Gamma(\cdot)$ is the Gamma function, $K_\nu(\cdot)$ is the modified Bessel function of the second kind, $\sigma^2 = \Gamma(\nu)/(\tau^2 \kappa^{2\nu} (4\pi)^{1/2} \Gamma(\nu + 1/2))$ is the marginal variance, $\kappa > 0$ is a parameter that controls the practical correlation range $\rho = \sqrt{8\nu}/\kappa$, and $0 < \nu = \alpha - 1/2$ is the smoothness parameter. Then the covariance function on the interval $[0, L]$ is

$$C_{\mathcal{N}}(s_1, s_2) = \sum_{k=-\infty}^{\infty} C(s_1 - s_2 + 2kL) + C(s_1 + s_2 + 2kL)$$

and the covariance function over a circle with arc-length parameterization on $[0, L]$ is

$$C_{\mathcal{P}}(s_1, s_2) = \sum_{k=-\infty}^{\infty} C(s_1 - s_2 + 2kL).$$

We remark that these infinite sums are not considered for numerical experiments but rather a truncated version of them. In the case of the tadpole graph, because the eigenpairs of the graph Laplacian Δ_Γ are known, the corresponding covariance function can be obtained using a truncated version of its Mercer representation (Steinwart and Scovel, 2012), retaining only a finite number of terms in the summation. Let $\Gamma_T = (\mathcal{V}, \mathcal{E})$ characterize the tadpole graph with $\mathcal{V} = \{v_1, v_2\}$ and $\mathcal{E} = \{e_1, e_2\}$ as specified in Figure 7c. The left edge e_1 has length 1 and the circular edge e_2 has length 2. As discussed in Subsection 2.1, a point on e_1 is parameterized via $s = (e_1, t)$ for $t \in [0, 1]$ and a point on e_2 via $s = (e_2, t)$ for $t \in [0, 2]$. One can verify that $-\Delta_\Gamma$ has eigenvalues $0, \{(i\pi/2)^2\}_{i \in \mathbb{N}}$ and $\{(i\pi/2)^2\}_{2i \in \mathbb{N}}$ with corresponding eigenfunctions $\phi_0, \{\phi_i\}_{i \in \mathbb{N}}$, and $\{\psi_i\}_{2i \in \mathbb{N}}$ given by $\phi_0(s) = 1/\sqrt{3}$ and

$$\phi_i(s) = C_{\phi,i} \begin{cases} -2 \sin\left(\frac{i\pi}{2}\right) \cos\left(\frac{i\pi t}{2}\right), & s \in e_1, \\ \sin(i\pi t/2), & s \in e_2, \end{cases}, \quad \psi_i(s) = \frac{\sqrt{3}}{\sqrt{2}} \begin{cases} (-1)^{i/2} \cos\left(\frac{i\pi t}{2}\right), & s \in e_1, \\ \cos\left(\frac{i\pi t}{2}\right), & s \in e_2, \end{cases},$$

where $C_{\phi,i} = 1$ if i is even and $C_{\phi,i} = 1/\sqrt{3}$ otherwise. Moreover, these functions form an orthonormal basis for $L_2(\Gamma_T)$.

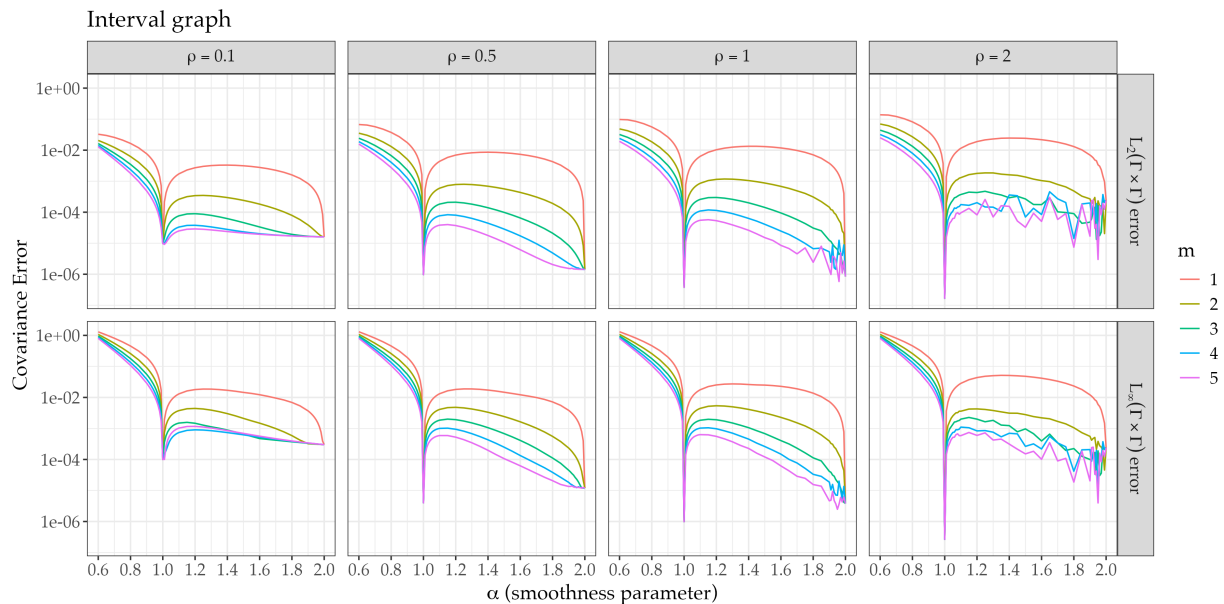


Figure 14: Errors in $L_2(\Gamma \times \Gamma)$ -norm (top row) and supremum norm (bottom row) on the interval graph for different combinations of parameters ρ (practical range), ν (smoothness), and m (rational order). In all cases, the FEM mesh contains 1000 equally spaced nodes.

J Error of the approximation

This section shows illustrations of the approximation errors for the interval and circle graphs. The choice of parameters is the same as in Section 4. Specifically, the errors for the interval case are shown in Figure 14 and the errors for the circle in Figure 15.

References

- Anderes, E., J. Møller, and J. G. Rasmussen (2020). Isotropic covariance functions on graphs and their edges. *Ann. Statist.* *48*(4), 2478–2503.
- Arioli, M. and M. Benzi (2018). A finite element method for quantum graphs. *IMA J. Numer. Anal.* *38*(3), 1119–1163.
- Bachl, F. E., F. Lindgren, D. L. Borchers, and J. B. Illian (2019). inlabru: an R package for Bayesian spatial modelling from ecological survey data. *Methods Ecol. Evol.* *10*, 760–766.
- Berkolaiko, G. and P. Kuchment (2013). *Introduction to quantum graphs*, Volume 186 of *Mathematical Surveys and Monographs*. American Mathematical Society, Providence, RI.
- Bogachev, V. I. (1998). *Gaussian Measures*, Volume 62 of *Mathematical Surveys and Monographs*. American Mathematical Society.
- Bolin, D. and K. Kirchner (2020). The rational SPDE approach for Gaussian random fields with general smoothness. *J. Comput. Graph. Statist.* *29*(2), 274–285.

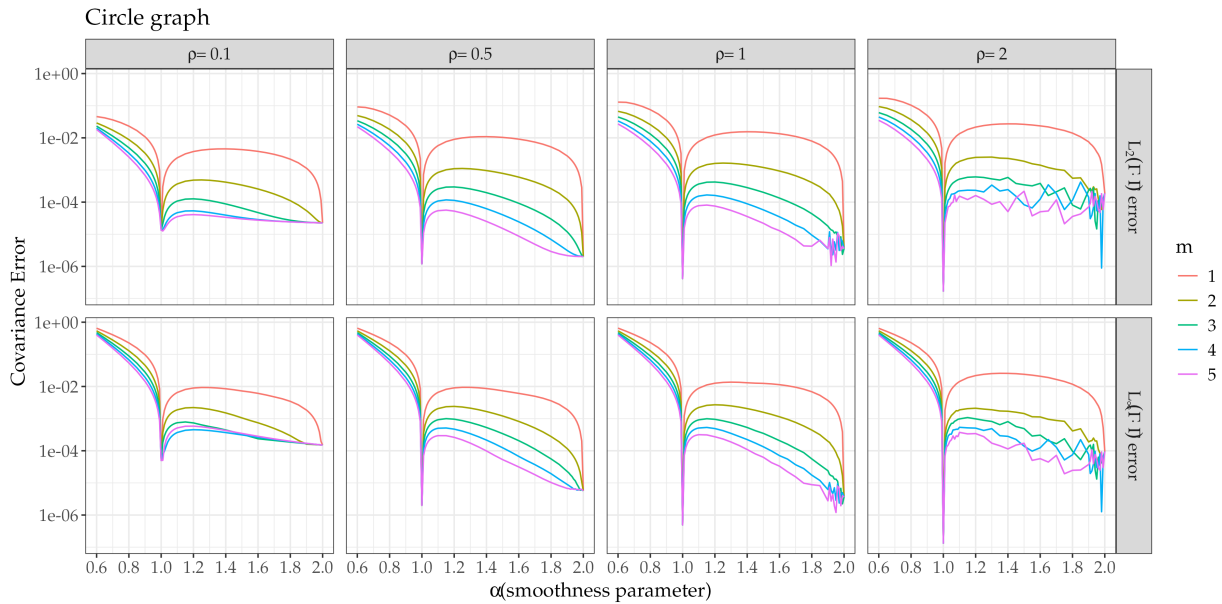


Figure 15: Errors in $L_2(\Gamma \times \Gamma)$ -norm (top row) and supremum norm (bottom row) on the circle graph for different combinations of parameters ρ (practical range), ν (smoothness), and m (rational order). In all cases, the FEM mesh contains 2000 equally spaced nodes.

Bolin, D., M. Kovács, V. Kumar, and A. B. Simas (2024). Regularity and numerical approximation of fractional elliptic differential equations on compact metric graphs. *Math. Comp.* 93(349), 2439–2472.

Bolin, D., A. Simas, and J. Wallin (2023a). Statistical inference for Gaussian Whittle-Matérn fields on metric graphs. Preprint arXiv:2304.10372.

Bolin, D. and A. B. Simas (2023). *rSPDE: Rational Approximations of Fractional Stochastic Partial Differential Equations*. R package version 2.4.0.

Bolin, D., A. B. Simas, and J. Wallin (2023b). *INLA interface for Whittle-Matérn fields on metric graphs*. In *MetricGraph: Random fields on metric graphs*, Version 1.4.0. https://davidbolin.github.io/MetricGraph/articles/inla_interface.html.

Bolin, D., A. B. Simas, and J. Wallin (2023c). *inlabru interface of Whittle-Matérn fields*. In *MetricGraph: Random fields on metric graphs*, Version 1.4.0. https://davidbolin.github.io/MetricGraph/articles/inlabru_interface.html.

Bolin, D., A. B. Simas, and J. Wallin (2023d). *MetricGraph: Random fields on metric graphs*. R package version 1.4.0.

Bolin, D., A. B. Simas, and J. Wallin (2024a). Gaussian Whittle-Matérn fields on metric graphs. *Bernoulli* 30(2), 1611–1639.

Bolin, D., A. B. Simas, and J. Wallin (2024b). Markov properties of Gaussian random fields on compact metric graphs. *Bernoulli*. Accepted for publication.

- Bolin, D., A. B. Simas, and Z. Xiong (2024). Covariance-based rational approximations of fractional SPDEs for computationally efficient Bayesian inference. *J. Comput. Graph. Statist.* 33(1), 64–74.
- Borovitskiy, V., I. Azangulov, A. Terenin, P. Mostowsky, M. Deisenroth, and N. Durrande (2021, 13–15 Apr). Matérn Gaussian Processes on Graphs. In A. Banerjee and K. Fukumizu (Eds.), *Proceedings of The 24th International Conference on Artificial Intelligence and Statistics*, Volume 130 of *Proceedings of Machine Learning Research*, pp. 2593–2601.
- Chen, C., K. Petty, A. Skabardonis, P. Varaiya, and Z. Jia (2001). Freeway performance measurement system: Mining loop detector data. *Transp. Res. Rec.* 1748(1), 96–102.
- Cressie, N., J. Frey, B. Harch, and M. Smith (2006, Jun). Spatial prediction on a river network. *J. Agric. Biol. Environ. Stat.* 11(2), 127.
- De Oliveira, V. and Z. Han (2022). On information about covariance parameters in Gaussian Matérn random fields. *J. Agric. Biol. Environ. Stat.* 27(4), 690–712.
- Filosi, T., C. Agostinelli, and E. Porcu (2023). Temporally-Evolving Generalised Networks and their Reproducing Kernels. Preprint arXiv:2309.15855.
- Fiorenza, R. (2017). *Hölder and locally Hölder Continuous Functions, and Open Sets of Class C^k , $C^{k,\lambda}$* . Birkhäuser Cham.
- Geoga, C. J., O. Marin, M. Schanen, and M. L. Stein (2023). Fitting Matérn smoothness parameters using automatic differentiation. *Stat. Comput.* 33(2), Paper No. 48, 16.
- Good, I. J. (1952). Rational decisions. *J. Roy. Statist. Soc. Ser. B* 14, 107–114.
- Hofreither, C. (2021). An algorithm for best rational approximation based on barycentric rational interpolation. *Numer. Algorithms* 88(1), 365–388.
- Janson, S. (1997). *Gaussian Hilbert Spaces*. Cambridge Tracts in Mathematics. Cambridge University Press.
- Khristenko, U., L. Scarabosio, P. Swierczynski, E. Ullmann, and B. Wohlmuth (2019). Analysis of boundary effects on PDE-based sampling of Whittle-Matérn random fields. *SIAM/ASA J. Uncertain. Quantif.* 7(3), 948–974.
- Kirchner, K. and D. Bolin (2022). Necessary and sufficient conditions for asymptotically optimal linear prediction of random fields on compact metric spaces. *Ann. Statist.* 50(2), 1038–1065.
- Lindgren, F. and H. Rue (2015). Bayesian Spatial Modelling with R-INLA. *J. Stat. Softw.* 63(19), 1–25.
- Lindgren, F., H. v. Rue, and J. Lindström (2011). An explicit link between Gaussian fields and Gaussian Markov random fields: the stochastic partial differential equation approach. *J. R. Stat. Soc. Ser. B Stat. Methodol.* 73(4), 423–498.

- Liu, Z. and H. Rue (2024). Leave-group-out cross-validation for latent Gaussian models. Preprint arXiv:2210.04482.
- Matérn, B. (1960). *Spatial variation: Stochastic models and their application to some problems in forest surveys and other sampling investigations*. Statens Skogsforskningsinstitut, Stockholm. Meddelanden Fran Statens Skogsforskningsinstitut, Band 49, Nr. 5.
- Møller, J. and J. G. Rasmussen (2024). Cox processes driven by transformed Gaussian processes on linear networks—a review and new contributions. *Scand. J. Stat.* 51(3), 1288–1322.
- OpenStreetMap contributors (2017). Planet dump retrieved from <https://planet.osm.org>. <https://www.openstreetmap.org>.
- Porcu, E., P. A. White, and M. G. Genton (2023). Stationary nonseparable space-time covariance functions on networks. *J. R. Stat. Soc. Ser. B. Stat. Methodol.* 85(5), 1417–1440.
- Sanz-Alonso, D. and R. Yang (2022). The SPDE Approach to Matérn Fields: Graph Representations. *Statist. Sci.* 37(4), 519–540.
- Stahl, H. R. (2003). Best uniform rational approximation of x^α on $[0, 1]$. *Acta Math.* 190(2), 241–306.
- Stein, M. L. (1999). *Interpolation of Spatial Data: Some Theory for Kriging*. Springer Series in Statistics. New York: Springer-Verlag.
- Steinwart, I. and C. Scovel (2012). Mercer’s theorem on general domains: on the interaction between measures, kernels, and RKHSs. *Constr. Approx.* 35(3), 363–417.
- Takahashi, K., J. Fagan, and M. S. Chin (1973). Formation of a sparse bus impedance matrix and its application to short circuit theory. *8th PICA Conf. Proc.*, 63–69.
- Ver Hoef, J. M., E. Peterson, and D. Theobald (2006). Spatial statistical models that use flow and stream distance. *Environ. Ecol. Stat.* 13(4), 449–464.